Flutter speed prediction of double-sweep folding wing in subsonic airflow

Shahrokh Shams[1*], Peyman Falahati[2], Mortaza Salehian[3]

[1]Associate Professor, School of Aerospace Engineering, College of Interdisciplinary Science and Technology, University of Tehran, North Kargar Street, Tehran, Iran, P.O.box: 1439957131

[2]Master, School of Aerospace Engineering, College of Interdisciplinary Science and Technology, University of Tehran, North Kargar Street, Tehran, Iran, P.O.box: 1439957131

[3]PhD candidate, Aerospace Engineering Dept. and Centre of Excellence in Computational Aerospace Engineering, Amirkabir University of Technology, Tehran, Iran

*Corresponding author' Email: shahrokh.shams@ut.ac.ir

Abstract:

This study addresses the prediction of the flutter speed for a double-sweep folding wing in subsonic airflow, an area less explored in past research. Two types of modeling are employed: structural and aerodynamic. The structural model treats the wing as an Euler-Bernoulli beam. For the aerodynamic model, Theodorsen's unsteady aerodynamic theory is used. This theory is initially in the frequency domain but is converted to the time domain using the Kussner function and a new formulation method. Kinetic energy, strain energy, and the work of aerodynamic forces are then calculated. The differential equations governing the wing structure are derived using Hamilton's principle. The wing's motion equation is obtained using assumed modes and the Galerkin method. The instability flutter speed is determined through the p-method, and graphs of frequency versus airflow velocity are plotted. The results indicate that using the Kussner function for variable airflow improves the accuracy of flutter speed prediction. The analysis of sweep angle changes on flutter speed and frequency revealed that sweep angle one has the least positive effect, while sweep angle two has the most positive effect on flutter speed and frequency, respectively.

Keywords: double-sweep, folding wing, aeroelastic, kussner, theodorsen

1- Introduction

Investigating the flutter phenomenon in wings is critical, as failure to accurately predict flutter speed can lead to severe oscillations that compromise wing integrity and aircraft stability. This investigation is particularly crucial for double-sweep folding wings, which frequently encounter variable airflow conditions that significantly impact their stability and aerodynamic performance. Consequently, predicting flutter speed and developing safe designs for these wings is essential. Furthermore, the distinctive design of double-sweep folding wings engenders unique aerodynamic characteristics that differ from the traditional wings, necessitating comprehensive analysis to optimize their design and functionality.

Borglund presented a novel method for robust flutter analysis, focusing on frequency-domain aerodynamics and structured singular value analysis [1]. Rajamurugu employed aerodynamic strip theory to analyze the static aeroelastic behavior of a slender straight 2D wing focusing on factors such as the distance between the elastic and aerodynamic axes, the sweep location, and the wing span [2]. Zhang et al. analyzed the transient response of advanced rotational variable-swept missile wings using a time-varying aeroelastic model. [3]. Dhital et al. explored the impact of aerodynamic interactions on the aeroelastic behavior of closely positioned wings, concluding that this arrangement offers superior aerodynamic efficiency compared to a single-wing configuration [4]. Farsadi et al. investigated the nonlinear dynamic aeroelasticity of composite thin-walled wings with circumferentially asymmetric layering in compressible flows [5]. Mazidi et al. investigated the aeroelastic behavior of swept wings of an aircraft equipped with two high-powered engines using Peter's aerodynamic model [6]. Sina et al. investigated the aeroelastic behavior of an anisotropic thin-walled composite beam in subsonic compressible flow [7]. Fazelzadeh et al. investigated the aeroelastic response of swept wings with shear deformation during roll [8]. Zhang et al. investigated the delta's leading-edge vortex effect on the wing's aerodynamic and aeroelastic characteristics [9]. Kapania et al. investigated the effect of variations in wing geometric parameters, including aspect ratio, wing surface area, taper ratio, and sweep angle, on the aeroelastic response of the wing in transonic airflow [10]. Ricketts investigated experimentally the aeroelastic behavior of forward-swept wings with different aspect ratios and sweep angles at low airspeed [11]. Mahig used the strip analysis method to determine the effect of flutter frequency and speed on variations in the drag coefficient and sweep angle and estimated wing stiffness through the strength of the material analysis [12]. Firouz-Abadi et al. investigated the stability of

aeroelastic models using a new reduced model. This model is designed based on identifying the generalized aerodynamic force response at different excitation frequencies [13]. Akshayraj et al. investigated the geometric variation of the wing on aerodynamic performance and flutter speed [14]. Kwon et al. predicted the unsteady flow vector of long wings in transonic flow using the unsteady potential equation of small supersonic turbulence [15]. Pollie et al. presented an analytical solution for the aeroelastic response of a swept wing made of advanced composite materials in incompressible subsonic flow, influenced by a time-dependent thermal field [16]. Ghasemikaram et al. presented a flutter analysis of a 3D aircraft with a box-wing configuration consisting of two front and rear wings connected to a central wing [17]. Fazelzadeh et al. presented the aeroelastic response of aircraft wings affected by changes in taper ratio, sweep angle, and variable pre-twist angle along the span [18]. Alizadeh et al. studied the aeroelastic and nonlinear flutter behavior of an externally stored cantilever wing experimentally in a closed-circuit subsonic wind tunnel [19]. Xiao et al. investigated the flutter analysis of a swept wing and considered the Theodorsen aerodynamic force variation using the Bisplinghoff aerodynamic force correction method as the aerodynamic model [20]. Basiri et al. achieved effective analysis and rapid modeling for free vibration and flutter analyses of low aspect ratio composite wings in subsonic flow [21]. Arun Kumar et al. analyzed the flutter of a sweptback wing and the effect of various parametric uncertainties using a frequency-domain aerodynamic model based on the structured singular value μ method [22]. Kumar et al. presented a physics-based algorithm for analyzing the reliability of aircraft wings in the frequency domain that uses the aeroelastic damping ratio of the flow velocity [23]. Melvin et al. presented a Ritz method for conducting the flutter analysis of a NASA X-57 Maxwell-like distributed propulsion aircraft wing including the bending displacement and torsion angle [24]. Liska et al. developed a continuous aeroelastic model for a folding wing, focusing on a uniform two-section wing with a hinge connecting the inner and outer sections [25]. Zhao et al. presented a parametric method for aeroelastic modeling that efficiently predicts the flutter characteristics of a folding wing [26]. Shams et al. conducted an aeroelastic analysis for a double-swept wing with metal/composite sections, which included investigating flutter, divergence, and aeroelastic static control [27]. Koo proposed a novel double-swept wing to enhance aeroelastic stability while maintaining aerodynamic advantages [28]. Marzocca et al. used the aerodynamic index function concept to present an integrated analysis of the aeroelastic dynamic response of sweep lifting surfaces in the time and frequency domains, which addresses time-dependent

external loads [29]. Mazidi et al. conducted a comprehensive flutter analysis of swept aircraft wings carrying a powered engine [30]. Firouz-Abadi et al. investigated the aeroelastic stability of subsonic tapered composite wings with two engines, considering the influence of engine thrust [31]. Sina et al. analyzed the aeroelastic stability and response of a composite swept wing in compressible subsonic flow [32]. Ovesy et al. conducted a study to analyze the effects of geometric structural nonlinearity on the flutter of high-aspect-ratio wings using ONERA aerodynamic model [33]. Jacobson et al. implemented and validated a frequency-domain linearized method in a stabilized finite element solver in FUN3D for flutter analysis in aeroelasticity [34]. Shi et al. presented a study on the aerodynamic analysis of airfoils, focusing on the accurate representation of the wake and the trailing edge condition [35].

The flutter speed of a double-sweep folding wing in subsonic airflow is determined in this paper. Certain small UAVs deploy their wings within seconds upon takeoff, which is why they are referred to as "folding wings." In this state, the airflow velocity is variable, leading to a different analysis of the flutter phenomenon compared to that of fixed wings. Therefore, Kussner's function is utilized instead of Wagner's function. This topic has not been explored in prior research, and this paper seeks to address this gap in the literature. The wing structure is modeled as a cantilever Euler-Bernoulli beam with two degrees of freedom: bending and torsion. The aerodynamic model of the airflow is described by using Theodorsen's unsteady aerodynamics. Kussner's function and a novel mathematical method convert the frequency domain to the time domain. Hamilton's principle is applied to derive the aeroelastic differential equation of the wing. The equation of motion for the wing is obtained by utilizing the Galerkin method and assumed modes. The p-method is then used to determine the flutter speed and frequency. Additionally, a design of experiments is conducted using the response surface method to analyze the impact of sweep angles on flutter speed and frequency, and the correlation matrix is generated. This paper highlights two significant achievements. First, utilizing Kussner's function in place of Wagner's function markedly enhances the accuracy of flutter speed and frequency calculation. Second, the impact of the sweep angle further from the body on flutter speed is greater than that of the sweep angle closer to the body.

2- Structural modeling

In this segment, the equation formula dictating the motion of the wing structure is derived under the premise of employing the Euler-Bernoulli beam theory. Subsequently, assessments of the strain energy, kinetic energy, and the effects of aerodynamic forces are conducted for the designated beams. Leveraging Hamilton's principle, the differential equation representing the structural dynamics of the beam is derived. Furthermore, employing the Galerkin and assumed modes methods, the governing equation for the beams' motion is deduced. Illustrated in Fig. 1 is a depiction of a wing featuring double sweeps, while Fig. 2 presents a schematic of its airfoil's cross-section.

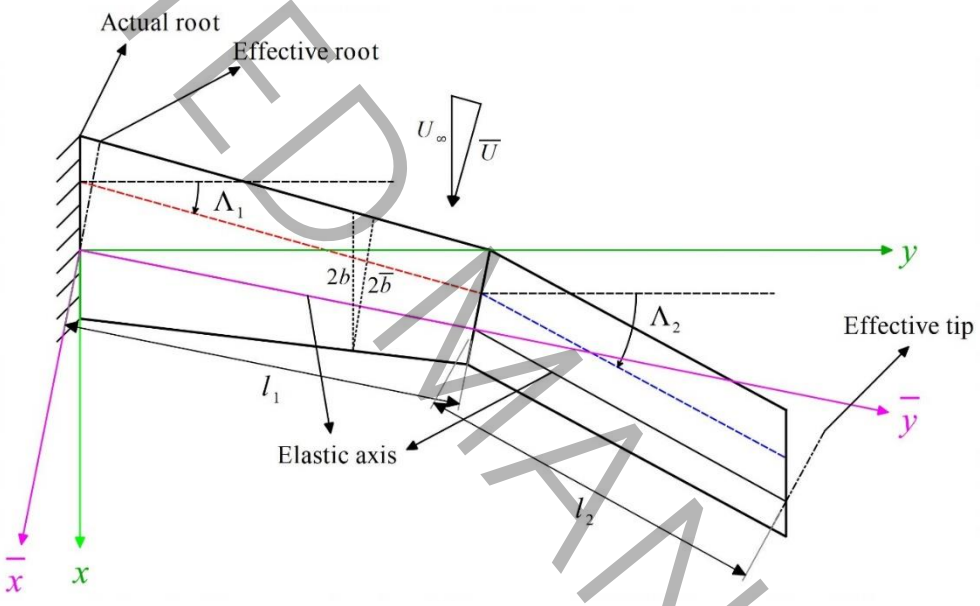

Fig. 1. Double sweep wing

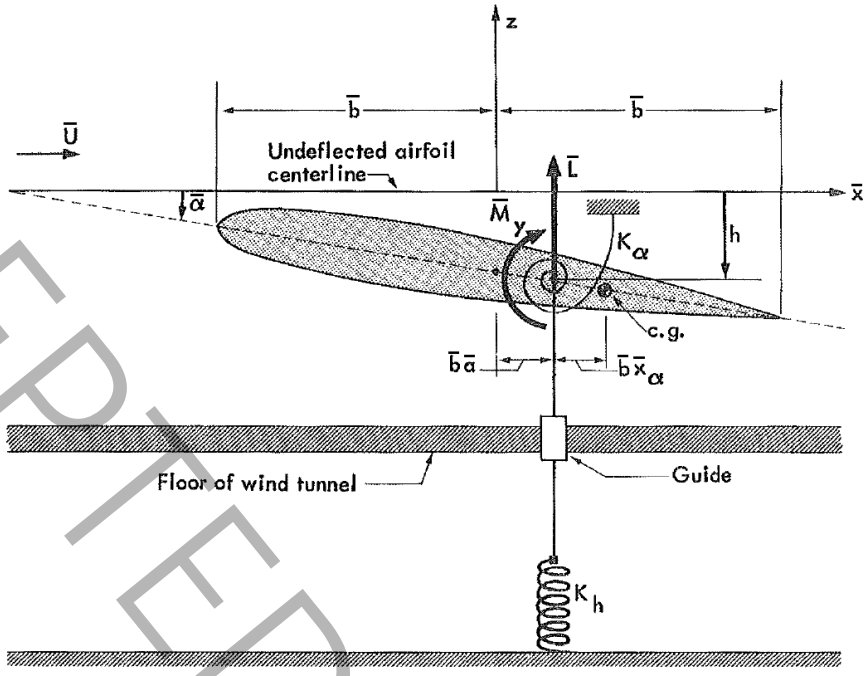

Fig. 2. Airfoil cross-section [36]

In Fig. 2, $\bar{b}$ represents half the wing chord length, $\bar{b}\bar{a}$ denotes the distance from the semi-chord to the elastic center, and $\bar{b}\bar{x}_{\alpha}$ signifies the distance from the elastic center to the center of mass. These distances are all measured perpendicular to the wing's elastic axis. As depicted in Figure 3, the wing structure manifests as an oblique two-part beam with independent coordinate systems.

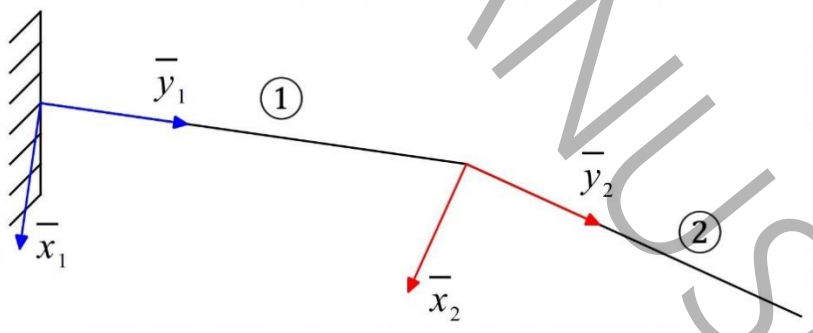

Fig. 3. Local coordinate systems of double beams

Strain energy with bending stiffness $\overline{EI}$ and torsional stiffness $\overline{GJ}$ is expressed as follows [37].

$$
\begin{aligned}
U &= U_1 + U_2 \\
&= \frac{1}{2}\cdot\int_0^{l_1}\left[\overline{EI_1}\cdot\left(\frac{\partial^2 w_1}{\partial \bar{y}_1^2}\right)^2 + \overline{GJ_1}\cdot\left(\frac{\partial \bar{\alpha}_1}{\partial \bar{y}_1}\right)^2\right]\cdot d\bar{y}_1 \\
&+\frac{1}{2}\cdot\int_0^{l_2}\left[\overline{EI_2}\cdot\left(\frac{\partial^2 w_2}{\partial \bar{y}_2^2}\right)^2 + \overline{GJ_2}\cdot\left(\frac{\partial \bar{\alpha}_2}{\partial \bar{y}_2}\right)^2\right]\cdot d\bar{y}_2
\end{aligned}
\tag{1}
$$

Where w and α represent the beam's bending and torsion degrees of freedom, and l_1 and l_2 denote the lengths of beams 1 and 2, respectively. By accounting for the mass density, the kinetic energy of the structure illustrated in Fig. 3 can be articulated as follows [37].

$$
\begin{aligned}
T &= \frac{1}{2}\cdot\int_0^{l_1}\left[\bar{m}_1\cdot\dot{w}_1^{\,2} - 2\cdot\bar{m}_1\cdot\bar{b}_1\cdot\bar{x}_{\alpha_1}\cdot\dot{w}_1\cdot\dot{\bar{\alpha}}_1 + \bar{I}_{\alpha_1}\cdot\dot{\bar{\alpha}}_1^2\right]\cdot d\bar{y}_1 \\
&+\frac{1}{2}\cdot\int_0^{l_2}\left[\bar{m}_2\cdot\dot{w}_2^{\,2} - 2\cdot\bar{m}_2\cdot\bar{b}_2\cdot\bar{x}_{\alpha_2}\cdot\dot{w}_2\cdot\dot{\bar{\alpha}}_2 + \bar{I}_{\alpha_2}\cdot\dot{\bar{\alpha}}_2^2\right]\cdot d\bar{y}_2
\end{aligned}
\tag{2}
$$

The variable $\bar{m}$ represents the mass per unit length, while $\bar{I}_\alpha$ denotes the mass moment of inertia of the wing's cross-section per unit length about the elastic axis. Furthermore, the virtual work done by aerodynamic forces is given by [37].

$$
W_{ext} = \int_0^{l_1}\left(\bar{L}_1\cdot w_1 + \bar{M}_{e.a_1}\cdot\bar{\alpha}_1\right)\cdot d\bar{y}_1 + \int_0^{l_2}\left(\bar{L}_2\cdot w_2 + \bar{M}_{e.a_2}\cdot\bar{\alpha}_2\right)\cdot d\bar{y}_2 \tag{3}
$$

In this context, $\bar{L}$ and $\bar{M}_{e.a}$ represent the aerodynamic force and aerodynamic moment, respectively, acting per unit length of the wing about its elastic center. The deriving governing equations for the wing can be derived by applying Eq. (1), (2), and (3) within the following framework of Hamilton's principle.

$$
\int\left(\delta U - \delta T\right)\cdot dt = \int \delta W_{ext}\cdot dt \tag{4}
$$

Applying the variational operator δ to the strain energy, kinetic energy, and external work yields the following result.

$$
\begin{aligned}
\delta U &= \int_0^{l_1}\left[\overline{EI_1}\cdot\frac{\partial^2 w_1}{\partial \bar{y}_1^2}\cdot\delta\left(\frac{\partial^2 w_1}{\partial \bar{y}_1^2}\right) + \overline{GJ_1}\cdot\left(\frac{\partial \bar{\alpha}_1}{\partial \bar{y}_1}\right)\cdot\delta\left(\frac{\partial \bar{\alpha}_1}{\partial \bar{y}_1}\right)\right]\cdot d\bar{y}_1 \\
&+\int_0^{l_2}\left[\overline{EI_2}\cdot\frac{\partial^2 w_2}{\partial \bar{y}_2^2}\cdot\delta\left(\frac{\partial^2 w_2}{\partial \bar{y}_2^2}\right) + \overline{GJ_2}\cdot\left(\frac{\partial \bar{\alpha}_2}{\partial \bar{y}_2}\right)\cdot\delta\left(\frac{\partial \bar{\alpha}_2}{\partial \bar{y}_2}\right)\right]\cdot d\bar{y}_2
\end{aligned}
\tag{5}
$$

$$
\begin{aligned}
\delta T &= \int_0^{l_1}\left\{\bar{m}_1\cdot\dot{w}_1\cdot\delta\dot{w}_1-\bar{m}_1\cdot\bar{b}_1\cdot\bar{x}_{\alpha_1}\cdot\left(\dot{w}_1\cdot\delta\dot{\bar{\alpha}}_1+\dot{\bar{\alpha}}_1\cdot\delta\dot{w}_1\right)+\bar{I}_{\alpha_1}\cdot\dot{\bar{\alpha}}_1\cdot\delta\dot{\bar{\alpha}}_1\right\}\cdot d\bar{y}_1\\
&+\int_0^{l_2}\left\{\bar{m}_2\cdot\dot{w}_2\cdot\delta\dot{w}_2-\bar{m}_2\cdot\bar{b}_2\cdot\bar{x}_{\alpha_2}\cdot\left(\dot{w}_2\cdot\delta\dot{\bar{\alpha}}_2+\dot{\bar{\alpha}}_2\cdot\delta\dot{w}_2\right)+\bar{I}_{\alpha_2}\cdot\dot{\bar{\alpha}}_2\cdot\delta\dot{\bar{\alpha}}_2\right\}\cdot d\bar{y}_2\\
&=-\int_0^{l_1}\left\{\bar{m}_1\cdot\ddot{w}_1\cdot\delta w_1-\bar{m}_1\cdot\bar{b}_1\cdot\bar{x}_{\alpha_1}\cdot\left(\ddot{w}_1\cdot\delta\bar{\alpha}_1+\ddot{\bar{\alpha}}_1\cdot\delta w_1\right)+\bar{I}_{\alpha_1}\cdot\ddot{\bar{\alpha}}_1\cdot\delta\bar{\alpha}_1\right\}\cdot d\bar{y}_1\\
&-\int_0^{l_2}\left\{\bar{m}_2\cdot\ddot{w}_2\cdot\delta w_2-\bar{m}_2\cdot\bar{b}_2\cdot\bar{x}_{\alpha_2}\cdot\left(\ddot{w}_2\cdot\delta\bar{\alpha}_2+\ddot{\bar{\alpha}}_2\cdot\delta w_2\right)+\bar{I}_{\alpha_2}\cdot\ddot{\bar{\alpha}}_2\cdot\delta\bar{\alpha}_2\right\}\cdot d\bar{y}_2\\
&=-\int_0^{l_1}\left\{\left(\bar{m}_1\cdot\ddot{w}_1-\bar{m}_1\cdot\bar{b}_1\cdot\bar{x}_{\alpha_1}\cdot\ddot{\bar{\alpha}}_1\right)\cdot\delta w_1+\left(\bar{I}_{\alpha_1}\cdot\ddot{\bar{\alpha}}_1-\bar{m}_1\cdot\bar{b}_1\cdot\bar{x}_{\alpha_1}\cdot\ddot{w}_1\right)\cdot\delta\bar{\alpha}_1\right\}\cdot d\bar{y}_1\\
&-\int_0^{l_2}\left\{\left(\bar{m}_2\cdot\ddot{w}_2-\bar{m}_2\cdot\bar{b}_2\cdot\bar{x}_{\alpha_2}\cdot\ddot{\bar{\alpha}}_2\right)\cdot\delta w_2+\left(\bar{I}_{\alpha_2}\cdot\ddot{\bar{\alpha}}_2-\bar{m}_2\cdot\bar{b}_2\cdot\bar{x}_{\alpha_2}\cdot\ddot{w}_2\right)\cdot\delta\bar{\alpha}_2\right\}\cdot d\bar{y}_2
\end{aligned}
\tag{6}
$$

$$
\delta W_{ext}=\int_0^{l_1}\left(\bar{L}_1\cdot\delta w_1+\bar{M}_{e.a_1}\cdot\delta\bar{\alpha}_1\right)\cdot d\bar{y}_1+\int_0^{l_2}\left(\bar{L}_2\cdot\delta w_2+\bar{M}_{e.a_2}\cdot\delta\bar{\alpha}_2\right)\cdot d\bar{y}_2 \tag{7}
$$

Therefore

$$
\begin{aligned}
&\int_0^{l_1}\left\{\begin{array}{l}\delta\left(\dfrac{\partial^2 w_1}{\partial\bar{y}_1^2}\right)\cdot\overline{EI}_1\cdot\left(\dfrac{\partial^2 w_1}{\partial\bar{y}_1^2}\right)+\delta\left(\dfrac{\partial\bar{\alpha}_1}{\partial\bar{y}_1}\right)\cdot\overline{GJ}_1\cdot\left(\dfrac{\partial\bar{\alpha}_1}{\partial\bar{y}_1}\right)\\+\delta w_1\cdot\left(\bar{m}_1\cdot\ddot{w}_1+\bar{m}_1\cdot\bar{b}_1\cdot\bar{x}_{\alpha_1}\cdot\ddot{\bar{\alpha}}_1\right)+\delta\bar{\alpha}_1\cdot\left(\bar{I}_{\alpha_1}\cdot\ddot{\bar{\alpha}}_1+\bar{m}_1\cdot\bar{b}_1\cdot\bar{x}_{\alpha_1}\cdot\ddot{w}_1\right)\end{array}\right\}\cdot d\bar{y}_1\\
&+\int_0^{l_2}\left\{\begin{array}{l}\delta\left(\dfrac{\partial^2 w_2}{\partial\bar{y}_2^2}\right)\cdot\overline{EI}_2\cdot\left(\dfrac{\partial^2 w_2}{\partial\bar{y}_2^2}\right)+\delta\left(\dfrac{\partial\bar{\alpha}_2}{\partial\bar{y}_2}\right)\cdot\overline{GJ}_2\cdot\left(\dfrac{\partial\bar{\alpha}_2}{\partial\bar{y}_2}\right)\\+\delta w_2\cdot\left(\bar{m}_2\cdot\ddot{w}_2+\bar{m}_2\cdot\bar{b}_2\cdot\bar{x}_{\alpha_2}\cdot\ddot{\bar{\alpha}}_2\right)+\delta\bar{\alpha}_2\cdot\left(\bar{I}_{\alpha_2}\cdot\ddot{\bar{\alpha}}_2+\bar{m}_2\cdot\bar{b}_2\cdot\bar{x}_{\alpha_2}\cdot\ddot{w}_2\right)\end{array}\right\}\cdot d\bar{y}_2\\
&=\int_0^{l_1}\left(\delta w_1\cdot\bar{L}_1+\delta\bar{\alpha}_1\cdot\bar{M}_{e.a_1}\right)\cdot d\bar{y}_1+\int_0^{l_2}\left(\delta w_2\cdot\bar{L}_2+\delta\bar{\alpha}_2\cdot\bar{M}_{e.a_2}\right)\cdot d\bar{y}_2
\end{aligned}
\tag{8}
$$

The degrees of freedom for bending and torsion are displayed as the mode shapes and generalized coordinates as follows.

$$
\begin{aligned}
w_1(\bar{y},t)&=\langle\Psi_1\rangle_{1\times N_w}\cdot\{r_w\}_{N_w\times 1}\quad;\qquad w_2(\bar{y},t)=\langle\Psi_2\rangle_{1\times N_w}\cdot\{r_w\}_{N_w\times 1}\\
\bar{\alpha}_1(\bar{y},t)&=\langle\Theta_1\rangle_{1\times N_{\bar{\alpha}}}\cdot\{r_{\bar{\alpha}}\}_{N_{\bar{\alpha}}\times 1}\quad;\qquad \bar{\alpha}_2(\bar{y},t)=\langle\Theta_2\rangle_{1\times N_{\bar{\alpha}}}\cdot\{r_{\bar{\alpha}}\}_{N_{\bar{\alpha}}\times 1}
\end{aligned}
\tag{9}
$$

The equation of motion is obtained using the assumed modes method in conjunction with the Galerkin method.

$$
\begin{aligned}
&\int_0^{l_1}\left\{\overline{EI_1}\cdot\{\Psi_1''\}\cdot\langle\Psi_1''\rangle\cdot\{r_w\}+\bar{m}_1\cdot\{\Psi_1\}\cdot\langle\Psi_1\rangle\cdot\{\ddot{r}_w\}-\bar{m}_1\cdot\bar{b}_1\cdot\bar{x}_{\alpha_1}\cdot\{\Psi_1\}\cdot\langle\Theta_1\rangle\cdot\{\ddot{r}_{\bar{\alpha}}\}\right\}\cdot d\bar{y}_1\\
&+\int_0^{l_2}\left\{\overline{EI_2}\cdot\{\Psi_2''\}\cdot\langle\Psi_2''\rangle\cdot\{r_w\}+\bar{m}_2\cdot\{\Psi_2\}\cdot\langle\Psi_2\rangle\cdot\{\ddot{r}_w\}-\bar{m}_2\cdot\bar{b}_2\cdot\bar{x}_{\alpha_2}\cdot\{\Psi_2\}\cdot\langle\Theta_2\rangle\cdot\{\ddot{r}_{\bar{\alpha}}\}\right\}\cdot d\bar{y}_2=\\
&\qquad\int_0^{l_1}\{\Psi_1\}\cdot\bar{L}_1\cdot d\bar{y}_1+\int_0^{l_2}\{\Psi_2\}\cdot\bar{L}_2\cdot d\bar{y}_2\\
&\int_0^{l_1}\left\{\overline{GJ_1}\cdot\{\Theta_1'\}\cdot\langle\Theta_1'\rangle\cdot\{r_{\bar{\alpha}}\}+\bar{I}_{\alpha_1}\cdot\{\Theta_1\}\cdot\langle\Theta_1\rangle\cdot\{\ddot{r}_{\bar{\alpha}}\}-\bar{m}_1\cdot\bar{b}_1\cdot\bar{x}_{\alpha_1}\cdot\{\Theta_1\}\cdot\langle\Psi_1\rangle\cdot\{\ddot{r}_w\}\right\}\cdot d\bar{y}_1\\
&+\int_0^{l_2}\left\{\{\Theta_2'\}\cdot\overline{GJ_2}\cdot\langle\Theta_2'\rangle\cdot\{r_{\bar{\alpha}}\}+\bar{I}_{\alpha_2}\cdot\{\Theta_2\}\cdot\langle\Theta_2\rangle\cdot\{\ddot{r}_{\bar{\alpha}}\}-\bar{m}_2\cdot\bar{b}_2\cdot\bar{x}_{\alpha_2}\cdot\{\Theta_2\}\cdot\langle\Psi_2\rangle\cdot\{\ddot{r}_w\}\right\}\cdot d\bar{y}_2=\\
&\qquad\int_0^{l_1}\{\Theta_1\}\cdot\bar{M}_{e.a_1}\cdot d\bar{y}_1+\int_0^{l_2}\{\Theta_2\}\cdot\bar{M}_{e.a_2}\cdot d\bar{y}_2
\end{aligned}
\tag{10}
$$

Ψ and Θ denote the mode shapes of bending and torsion, respectively, while r_w and r_α represents the generalized coordinates for bending and torsion, respectively. In general, the mode shapes for bending and torsion of both beams can be described as follows.

$$
\begin{aligned}
&\Theta_1(\bar{y}_1)=A_1\cdot\cos\left(\frac{\omega\cdot\bar{y}_1}{h}\right)+A_2\cdot\sin\left(\frac{\omega\cdot\bar{y}_1}{h}\right),\quad h=\sqrt{\frac{\overline{G}}{\rho}}\\
&\Theta_2(\bar{y}_2)=B_1\cdot\cos\left(\frac{\omega\cdot\bar{y}_2}{h}\right)+B_2\cdot\sin\left(\frac{\omega\cdot\bar{y}_2}{h}\right)\\
&\Psi_1(\bar{y}_1)=C_1\cdot\cos(\chi\cdot\bar{y}_1)+C_2\cdot\sin(\chi\cdot\bar{y}_1)+C_3\cdot\cosh(\chi\cdot\bar{y}_1)+C_4\cdot\sinh(\chi\cdot\bar{y}_1)\\
&\Psi_2(\bar{y}_2)=D_1\cdot\cos(\chi\cdot\bar{y}_2)+D_2\cdot\sin(\chi\cdot\bar{y}_2)+D_3\cdot\cosh(\chi\cdot\bar{y}_2)+D_4\cdot\sinh(\chi\cdot\bar{y}_2)
\end{aligned}
\tag{11}
$$

The boundary conditions of the beams lead to the following expressions. The connection point of beam 1 to the body is clamped, resulting in zero bending and torsion at this location. At the junction between the two beams, the bending and torsion, along with their first and second derivatives, are continuous and equal for both beams. The endpoint of beam 2 is free, where the first derivative of torsion, and the second and third derivatives of bending, are zero. Therefore, 12 boundary conditions are obtained.

$$\Psi_1(0)=0 \quad , \quad \Theta_1(0)=0 \quad , \quad \frac{\partial\Psi_1}{\partial\overline{y}_1}(0)=0$$

$$\Psi_1(l_1)=\Psi_2(0) \quad , \quad \Theta_1(l_1)=\Theta_2(0) \quad , \quad \frac{\partial\Theta_1}{\partial\overline{y}_1}(l_1)=\frac{\partial\Theta_2}{\partial\overline{y}_2}(0)$$

$$\frac{\partial\Psi_1}{\partial\overline{y}_1}(l_1)=\frac{\partial\Psi_2}{\partial\overline{y}_2}(0) \quad , \quad \frac{\partial^2\Psi_1}{\partial\overline{y}_1^2}(l_1)=\frac{\partial^2\Psi_2}{\partial\overline{y}_2^2}(0) \quad , \quad \frac{\partial^3\Psi_1}{\partial\overline{y}_1^3}(l_1)=\frac{\partial^3\Psi_2}{\partial\overline{y}_2^3}(0) \tag{12}$$

$$\frac{\partial\Theta_2}{\partial\overline{y}_2}(l_2)=0 \quad , \quad \frac{\partial^2\Psi_2}{\partial\overline{y}_2^2}(l_2)=0 \quad , \quad \frac{\partial^3\Psi_2}{\partial\overline{y}_2^3}(l_2)=0$$

By substituting Eq. (12) into Eq. (11) and solving a system of linear equations including twelve equations with twelve unknowns, the following results can be derived for the bending and torsion modes.

$$D_2=\frac{\cos(\chi\cdot l_1)}{\sin(\chi\cdot l_1)}$$

$$D_3=\frac{\sinh(\chi\cdot l_1)\cdot\left(-\sin(\chi\cdot l_1)\cdot\sin(\chi\cdot l_2)+\cos(\chi\cdot l_2)\cdot\cos(\chi\cdot l_1)\right)}{\sin(\chi\cdot l_1)\cdot\left(\cosh(\chi\cdot l_1)\cdot\cosh(\chi\cdot l_2)+\sinh(\chi\cdot l_1)\cdot\sinh(\chi\cdot l_2)\right)}$$

$$D_4=\frac{\cosh(\chi\cdot l_1)\cdot\left(-\sin(\chi\cdot l_1)\cdot\sin(\chi\cdot l_2)+\cos(\chi\cdot l_2)\cdot\cos(\chi\cdot l_1)\right)}{\sin(\chi\cdot l_1)\cdot\left(\cosh(\chi\cdot l_1)\cdot\cosh(\chi\cdot l_2)+\sinh(\chi\cdot l_1)\cdot\sinh(\chi\cdot l_2)\right)}$$

$$C_1=C_3=0 \tag{13}$$

$$C_2=\frac{1}{\sin(\chi\cdot l_1)}$$

$$C_4=\frac{-\sin(\chi\cdot l_1)\cdot\sin(\chi\cdot l_2)+\cos(\chi\cdot l_2)\cdot\cos(\chi\cdot l_1)}{\sin(\chi\cdot l_1)\cdot\left(\cosh(\chi\cdot l_1)\cdot\cosh(\chi\cdot l_2)+\sinh(\chi\cdot l_1)\cdot\sinh(\chi\cdot l_2)\right)}$$

$$A_1=0,\ A_2=1$$

$$B_1=\cos\left(\frac{\omega\cdot l_1}{h}\right)\cdot\cot\left(\frac{\omega\cdot l_2}{h}\right),\quad B_2=\cos\left(\frac{\omega\cdot l_1}{h}\right)$$

Consequently, the mode shapes of bending and torsion of beams are derived as follows.

$$\Psi_{1i}(\bar{y}_1)=\frac{1}{\sin(\chi_i\cdot l_1)}\cdot\sin(\chi_i\cdot\bar{y}_1)$$
$$+\frac{-\sin(\chi_i\cdot l_1)\cdot\sin(\chi_i\cdot l_2)+\cos(\chi_i\cdot l_2)\cdot\cos(\chi_i\cdot l_1)}{\sin(\chi_i\cdot l_1)\cdot\left(\cosh(\chi_i\cdot l_1)\cdot\cosh(\chi_i\cdot l_2)+\sinh(\chi_i\cdot l_1)\cdot\sinh(\chi_i\cdot l_2)\right)}\cdot\sinh(\chi_i\cdot\bar{y}_1)$$
$$\Psi_{2i}(\bar{y}_2)=\cos(\chi_i\cdot\bar{y}_2)$$
$$+\frac{\cos(\chi_i\cdot l_1)}{\sin(\chi_i\cdot l_1)}\cdot\sin(\chi_i\cdot\bar{y}_2)$$
$$+\frac{\sinh(\chi_i\cdot l_1)\cdot\left(-\sin(\chi_i\cdot l_1)\cdot\sin(\chi_i\cdot l_2)+\cos(\chi_i\cdot l_2)\cdot\cos(\chi_i\cdot l_1)\right)}{\sin(\chi_i\cdot l_1)\cdot\left(\cosh(\chi_i\cdot l_1)\cdot\cosh(\chi_i\cdot l_2)+\sinh(\chi_i\cdot l_1)\cdot\sinh(\chi_i\cdot l_2)\right)}\cdot\cosh(\chi_i\cdot\bar{y}_2)$$
$$+\frac{\cosh(\chi_i\cdot l_1)\cdot\left(-\sin(\chi_i\cdot l_1)\cdot\sin(\chi_i\cdot l_2)+\cos(\chi_i\cdot l_2)\cdot\cos(\chi_i\cdot l_1)\right)}{\sin(\chi_i\cdot l_1)\cdot\left(\cosh(\chi_i\cdot l_1)\cdot\cosh(\chi_i\cdot l_2)+\sinh(\chi_i\cdot l_1)\cdot\sinh(\chi_i\cdot l_2)\right)}\cdot\sinh(\chi_i\cdot\bar{y}_2) \quad (14)$$

$$\Theta_{1i}(\bar{y}_1)=\sin(\omega_i\cdot\bar{y}_1)$$
$$\Theta_{2i}(\bar{y}_2)=\cos(\omega_i\cdot l_1)\cdot\cot(\omega_i\cdot l_2)\cdot\cos(\omega_i\cdot\bar{y}_2)+\cos(\omega_i\cdot l_1)\cdot\sin(\omega_i\cdot\bar{y}_2) \quad (15)$$

Where χ_i and ω_i are obtained from the following equations.

$$\cosh(\chi_i\cdot l_1)\cdot\sin(\chi_i\cdot l_1)=0$$
$$\tan(\omega_i\cdot l_1)\cdot\tan(\omega_i\cdot l_2)-1=0 \quad (16)$$

3- Aerodynamic Modeling

This section elucidates the equations governing lift force and aerodynamic moment utilizing the assumed strip theory. Consequently, expressions for lift force and aerodynamic moment are formulated accordingly [38].

$$\bar{L}=\pi\cdot\rho_\infty\cdot\bar{b}^2\cdot\begin{bmatrix}-\ddot{w}+U_\infty\cdot\dot{\bar{\alpha}}\cdot\cos(\Lambda)-U_\infty\cdot\dot{w}'\cdot\sin(\Lambda)\\-\bar{b}\cdot\bar{a}\cdot\ddot{\bar{\alpha}}-\bar{b}\cdot\bar{a}\cdot U_\infty\cdot\dot{\bar{\alpha}}'\cdot\sin(\Lambda)\end{bmatrix}$$
$$+2\cdot\pi\cdot\rho_\infty\cdot U_\infty\cdot\cos(\Lambda)\cdot\bar{b}\cdot\left[w_a(0)\cdot\psi(t)+\int_0^t\psi(t-\tau)\cdot\frac{dw_a(\tau)}{d\tau}\cdot d\tau\right]$$
$$\bar{M}_{e.a}=-\pi\cdot\rho_\infty\cdot\bar{b}^3\cdot\begin{bmatrix}U_\infty\cdot\left(\frac{1}{2}-\bar{a}\right)\cdot\dot{\bar{\alpha}}\cdot\cos(\Lambda)+\frac{1}{2}\cdot U_\infty^2\cdot\bar{\alpha}'\cdot\cos(\Lambda)\cdot\sin(\Lambda)+\bar{a}\cdot\ddot{w}\\+U_\infty\cdot\bar{a}\cdot\dot{w}'\cdot\sin(\Lambda)+\bar{b}\cdot\left(\frac{1}{8}+\bar{a}^2\right)\cdot\left(\ddot{\bar{\alpha}}+U_\infty\cdot\dot{\bar{\alpha}}'\cdot\sin(\Lambda)\right)\end{bmatrix} \quad (17)$$
$$+2\cdot\pi\cdot\rho_\infty\cdot U_\infty\cdot\cos(\Lambda)\cdot\bar{b}\cdot\bar{e}\cdot\left[w_a(0)\cdot\psi(t)+\int_0^t\psi(t-\tau)\cdot\frac{dw_a(\tau)}{d\tau}\cdot d\tau\right]$$

Here, U_∞, ρ_∞, and Λ represent the airflow velocity, airflow density, and the wing sweep angle, respectively. The macron symbol ($\bar{}$) and the dot ($\dot{}$) above the letters indicate derivatives with respect to time and displacement in the y-direction, respectively. w_a is downwash velocity which is expressed as follows [39].

$$w_a = -\dot{w} + U_\infty \cdot \left(\bar{\alpha} \cdot \cos(\Lambda) - w' \cdot \sin(\Lambda)\right) + \bar{b} \cdot \left(\frac{1}{2} - \bar{a}\right) \cdot \left(\dot{\bar{\alpha}} + U_\infty \cdot \bar{\alpha}' \cdot \sin(\Lambda)\right) \tag{18}$$

And ψ is the Kussner's function is expressed as follows [38].

$$\begin{aligned} &\psi(t) = 1 - d \cdot e^{-\kappa_1 \cdot t} - d \cdot e^{-\kappa_2 \cdot t} \\ &d = 0.5, \quad \kappa_1 = 0.13 \cdot \frac{\bar{U}}{\bar{b}}, \quad \kappa_2 = \frac{\bar{U}}{\bar{b}} \end{aligned} \tag{19}$$

By substituting the downwash velocity from Eq. (18) into Eq. (17), the lift force and aerodynamic moment can be determined [39].

$$\begin{aligned} \bar{L} = {} & \pi \cdot \rho_\infty \cdot \bar{b}^2 \cdot \begin{bmatrix} -\ddot{w} + U_\infty \cdot \dot{\bar{\alpha}} \cdot \cos(\Lambda) - U_\infty \cdot \dot{w}' \cdot \sin(\Lambda) \\ -\bar{b} \cdot \bar{a} \cdot \ddot{\bar{\alpha}} - \bar{b} \cdot \bar{a} \cdot U_\infty \cdot \dot{\bar{\alpha}}' \cdot \sin(\Lambda) \end{bmatrix} \\ & + 2 \cdot \pi \cdot \rho_\infty \cdot U_\infty \cdot \cos(\Lambda) \cdot \bar{b} \cdot \begin{bmatrix} -\dot{w}(0) + U_\infty \cdot \left(\bar{\alpha}(0) \cdot \cos(\Lambda) - w'(0) \cdot \sin(\Lambda)\right) \\ +\bar{b} \cdot \left(\frac{1}{2} - \bar{a}\right) \cdot \left(\dot{\bar{\alpha}}(0) + U_\infty \cdot \bar{\alpha}'(0) \cdot \sin(\Lambda)\right) \end{bmatrix} \cdot \psi(t) \\ & + 2 \cdot \pi \cdot \rho_\infty \cdot U_\infty \cdot \cos(\Lambda) \cdot \bar{b} \cdot \int_0^t \psi(t-\tau) \cdot \begin{bmatrix} -\ddot{w} + U_\infty \cdot \left(\dot{\bar{\alpha}} \cdot \cos(\Lambda) - \dot{w}' \cdot \sin(\Lambda)\right) \\ +\bar{b} \cdot \left(\frac{1}{2} - \bar{a}\right) \cdot \left(\ddot{\bar{\alpha}} + U_\infty \cdot \dot{\bar{\alpha}}' \cdot \sin(\Lambda)\right) \end{bmatrix} \cdot d\tau \end{aligned}$$

$$\begin{aligned} \bar{M}_{e.a} = {} & -\pi \cdot \rho_\infty \cdot \bar{b}^3 \cdot \begin{bmatrix} U_\infty \cdot \left(\frac{1}{2} - \bar{a}\right) \cdot \dot{\bar{\alpha}} \cdot \cos(\Lambda) + \frac{1}{2} \cdot U_\infty^2 \cdot \bar{\alpha}' \cdot \cos(\Lambda) \cdot \sin(\Lambda) + \bar{a} \cdot \ddot{w} \\ +U_\infty \cdot \bar{a} \cdot \dot{w}' \cdot \sin(\Lambda) + \bar{b} \cdot \left(\frac{1}{8} + \bar{a}^2\right) \cdot \left(\ddot{\bar{\alpha}} + U_\infty \cdot \dot{\bar{\alpha}}' \cdot \sin(\Lambda)\right) \end{bmatrix} \\ & + 2 \cdot \pi \cdot \rho_\infty \cdot U_\infty \cdot \cos(\Lambda) \cdot \bar{b} \cdot \bar{e} \cdot \begin{bmatrix} -\dot{w}(0) + U_\infty \cdot \left(\bar{\alpha}(0) \cdot \cos(\Lambda) - w'(0) \cdot \sin(\Lambda)\right) \\ +\bar{b} \cdot \left(\frac{1}{2} - \bar{a}\right) \cdot \left(\dot{\bar{\alpha}}(0) + U_\infty \cdot \bar{\alpha}'(0) \cdot \sin(\Lambda)\right) \end{bmatrix} \cdot \psi(t) \\ & + 2 \cdot \pi \cdot \rho_\infty \cdot U_\infty \cdot \cos(\Lambda) \cdot \bar{b} \cdot \bar{e} \cdot \int_0^t \psi(t-\tau) \cdot \begin{bmatrix} -\ddot{w} + U_\infty \cdot \left(\dot{\bar{\alpha}} \cdot \cos(\Lambda) - \dot{w}' \cdot \sin(\Lambda)\right) \\ +\bar{b} \cdot \left(\frac{1}{2} - \bar{a}\right) \cdot \left(\ddot{\bar{\alpha}} + U_\infty \cdot \dot{\bar{\alpha}}' \cdot \sin(\Lambda)\right) \end{bmatrix} \cdot d\tau \end{aligned} \tag{20}$$

Considering the following variables, an innovative method can be formulated as follows:

$$\left[\frac{d}{dt}F_{w\alpha\alpha}\right]=\left[-\ddot{w}+U_\infty\cdot\left(\dot{\bar{\alpha}}\cdot\cos(\Lambda)-\dot{w}'\cdot\sin(\Lambda)\right)+\bar{b}\cdot\left(\frac{1}{2}-\bar{a}\right)\cdot\left(\ddot{\bar{\alpha}}+U_\infty\cdot\dot{\bar{\alpha}}'\cdot\sin(\Lambda)\right)\right]$$

$$\Rightarrow\left[F_{w\alpha\alpha}\right]=\left[-\dot{w}+U_\infty\cdot\left(\bar{\alpha}\cdot\cos(\Lambda)-w'\cdot\sin(\Lambda)\right)+\bar{b}\cdot\left(\frac{1}{2}-\bar{a}\right)\cdot\left(\dot{\bar{\alpha}}+U_\infty\cdot\bar{\alpha}'\cdot\sin(\Lambda)\right)\right]$$

$$=\left[\frac{d}{dt}F_{w\alpha}\right]+\left[U_\infty\cdot\left(\bar{\alpha}\cdot\cos(\Lambda)-w'\cdot\sin(\Lambda)\right)+\bar{b}\cdot\left(\frac{1}{2}-\bar{a}\right)\cdot U_\infty\cdot\bar{\alpha}'\cdot\sin(\Lambda)\right]$$

$$\left[\frac{d}{dt}F_{w\alpha}\right]=\left[-\dot{w}+\bar{b}\cdot\left(\frac{1}{2}-\bar{a}\right)\cdot\dot{\bar{\alpha}}\right]$$

$$\Rightarrow\left[F_{w\alpha}\right]=\left[-w+\bar{b}\cdot\left(\frac{1}{2}-\bar{a}\right)\cdot\bar{\alpha}\right] \tag{21}$$

$$\Rightarrow\left[U_\infty\cdot\left(\bar{\alpha}\cdot\cos(\Lambda)-w'\cdot\sin(\Lambda)\right)+\bar{b}\cdot\left(\frac{1}{2}-\bar{a}\right)\cdot U_\infty\cdot\bar{\alpha}'\cdot\sin(\Lambda)\right]-\kappa_i\cdot\left[F_{w\alpha}\right]$$

$$=\begin{bmatrix}U_\infty\cdot\bar{\alpha}\cdot\cos(\Lambda)+\bar{b}\cdot\left(\frac{1}{2}-\bar{a}\right)\cdot U_\infty\cdot\bar{\alpha}'\cdot\sin(\Lambda)\\-U_\infty\cdot w'\cdot\sin(\Lambda)\end{bmatrix}-\kappa_i\cdot\left[-w+\bar{b}\cdot\left(\frac{1}{2}-\bar{a}\right)\cdot\bar{\alpha}\right]$$

Eq. (21) introduces an innovative mathematical method for calculating Kussner's integral, which is further expanded upon in the paper. This approach is novel and has not been previously employed in any other work. Kussner's integral, presented in Eq. (20), can be expressed as follows.

$$\int_0^t\psi(t-\tau)\cdot\begin{bmatrix}-\ddot{w}+U_\infty\cdot\left(\dot{\bar{\alpha}}\cdot\cos(\Lambda)-\dot{w}'\cdot\sin(\Lambda)\right)\\+\bar{b}\cdot\left(\frac{1}{2}-\bar{a}\right)\cdot\left(\ddot{\bar{\alpha}}+U_\infty\cdot\dot{\bar{\alpha}}'\cdot\sin(\Lambda)\right)\end{bmatrix}\cdot d\tau=$$

$$\int_0^t\left(1-d\cdot e^{-\kappa_1\cdot(t-\tau)}-d\cdot e^{-\kappa_2\cdot(t-\tau)}\right)\cdot\left[\frac{d}{d\tau}F_{w\alpha\alpha}\right]\cdot d\tau= \tag{22}$$

$$\int_0^t\left[\frac{d}{d\tau}F_{w\alpha\alpha}\right]\cdot d\tau-d\cdot e^{-\kappa_1\cdot t}\cdot\int_0^t e^{\kappa_1\cdot\tau}\cdot\left[\frac{d}{d\tau}F_{w\alpha\alpha}\right]\cdot d\tau-d\cdot e^{-\kappa_2\cdot t}\cdot\int_0^t e^{\kappa_2\cdot\tau}\cdot\left[\frac{d}{d\tau}F_{w\alpha\alpha}\right]\cdot d\tau=$$

$$A_0-d\cdot e^{-\kappa_1\cdot t}\cdot A_1-d\cdot e^{-\kappa_2\cdot t}\cdot A_2$$

Where

$$A_0 = \left(F_{w\alpha\alpha}\right)\Big|_0^t = F_{w\alpha\alpha} - F_{w\alpha\alpha}\left(0\right)$$

$$A_i = \int_0^t e^{\kappa_i\cdot\tau}\cdot\left[\frac{d}{d\tau}F_{w\alpha\alpha}\right]\cdot d\tau = \left(e^{\kappa_i\cdot\tau}\cdot F_{w\alpha\alpha}\right)\Big|_0^t - \kappa_i\cdot\int_0^t e^{\kappa_i\cdot\tau}\cdot\left[F_{w\alpha\alpha}\right]\cdot d\tau$$

$$= \left(e^{\kappa_i\cdot\tau}\cdot F_{w\alpha\alpha}\right)\Big|_0^t - \kappa_i\cdot B_i$$

$$B_i = \int_0^t e^{\kappa_i\cdot\tau}\cdot\left[F_{w\alpha\alpha}\right]\cdot d\tau$$

$$= \int_0^t e^{\kappa_i\cdot\tau}\cdot\left(\begin{bmatrix}\frac{d}{d\tau}F_{w\alpha}\end{bmatrix} + \left[U_\infty\cdot\left(\bar{\alpha}\cdot\cos\left(\Lambda\right) - w'\cdot\sin\left(\Lambda\right)\right) + \bar{b}\cdot\left(\frac{1}{2}-\bar{a}\right)\cdot U_\infty\cdot\bar{\alpha}'\cdot\sin\left(\Lambda\right)\right]\right)\cdot d\tau$$

$$= \int_0^t e^{\kappa_i\cdot\tau}\cdot\left[\frac{d}{d\tau}F_{w\alpha}\right]\cdot d\tau + \int_0^t e^{\kappa_i\cdot\tau}\cdot\left[U_\infty\cdot\left(\bar{\alpha}\cdot\cos\left(\Lambda\right) - w'\cdot\sin\left(\Lambda\right)\right) + \bar{b}\cdot\left(\frac{1}{2}-\bar{a}\right)\cdot U_\infty\cdot\bar{\alpha}'\cdot\sin\left(\Lambda\right)\right]\cdot d\tau \quad (23)$$

$$= C_i + D_i$$

$$C_i = \int_0^t e^{\kappa_i\cdot\tau}\cdot\left[\frac{d}{d\tau}F_{w\alpha}\right]\cdot d\tau = \left(e^{\kappa_i\cdot\tau}\cdot F_{w\alpha}\right)\Big|_0^t - \kappa_i\cdot\int_0^t e^{\kappa_i\cdot\tau}\cdot\left[F_{w\alpha}\right]\cdot d\tau$$

$$= e^{\kappa_i\cdot t}\cdot F_{w\alpha} - F_{w\alpha}\left(0\right) - \kappa_i\cdot\int_0^t e^{\kappa_i\cdot\tau}\cdot\left[F_{w\alpha}\right]\cdot d\tau$$

$$D_i = \int_0^t e^{\kappa_i\cdot\tau}\cdot\left[U_\infty\cdot\left(\bar{\alpha}\cdot\cos\left(\Lambda\right) - w'\cdot\sin\left(\Lambda\right)\right) + \bar{b}\cdot\left(\frac{1}{2}-\bar{a}\right)\cdot U_\infty\cdot\bar{\alpha}'\cdot\sin\left(\Lambda\right)\right]\cdot d\tau$$

$$= \int_0^t e^{\kappa_i\cdot\tau}\cdot\left[U_\infty\cdot\bar{\alpha}\cdot\cos\left(\Lambda\right)\right]\cdot d\tau - \int_0^t e^{\kappa_i\cdot\tau}\cdot\left[U_\infty\cdot w'\cdot\sin\left(\Lambda\right)\right]\cdot d\tau$$

$$+\int_0^t e^{\kappa_i\cdot\tau}\cdot\bar{b}\cdot\left(\frac{1}{2}-\bar{a}\right)\cdot U_\infty\cdot\bar{\alpha}'\cdot\sin\left(\Lambda\right)\cdot d\tau$$

Inserting the Eq. (23) into the Eq. (22), it can be written.

$$d\cdot e^{-\kappa_i\cdot t}\cdot A_i = d\cdot F_{w\alpha\alpha} - d\cdot e^{-\kappa_i\cdot t}\cdot F_{w\alpha\alpha}\left(0\right) - \kappa_i\cdot d\cdot e^{-\kappa_i\cdot t}\cdot\left(C_i + D_i\right) \quad (24)$$

Therefore, Eq. (24) is rewritten as follows.

$$
\begin{aligned}
& d\cdot e^{-\kappa_i\cdot t}\cdot A_i = d\cdot F_{w\alpha\alpha} - d\cdot e^{-\kappa_i\cdot t}\cdot F_{w\alpha\alpha}\left(0\right) \\
& -\kappa_i\cdot d\cdot F_{w\alpha} + \kappa_i\cdot d\cdot e^{-\kappa_i\cdot t}\cdot F_{w\alpha}\left(0\right) + \kappa_i^2\cdot d\cdot e^{-\kappa_i\cdot t}\cdot\int_0^t e^{\kappa_i\cdot\tau}\cdot\left[F_{w\alpha}\right]\cdot d\tau \\
& -\kappa_i\cdot d\cdot e^{-\kappa_i\cdot t}\cdot\int_0^t e^{\kappa_i\cdot\tau}\cdot\left[U_\infty\cdot\bar{\alpha}\cdot\cos\left(\Lambda\right)\right]\cdot d\tau \\
& +\kappa_i\cdot d\cdot e^{-\kappa_i\cdot t}\cdot\int_0^t e^{\kappa_i\cdot\tau}\cdot\left[U_\infty\cdot w'\cdot\sin\left(\Lambda\right)\right]\cdot d\tau \\
& -\kappa_i\cdot d\cdot e^{-\kappa_i\cdot t}\cdot\int_0^t e^{\kappa_i\cdot\tau}\cdot\bar{b}\cdot\left(\frac{1}{2}-\bar{a}\right)\cdot U_\infty\cdot\bar{\alpha}'\cdot\sin\left(\Lambda\right)\cdot d\tau
\end{aligned}
\tag{25}
$$

Substituting Eq. (25) into Eq. (22) results in the following rewritten expression.

$$
\begin{aligned}
& \int_0^t\psi\left(t-\tau\right)\cdot\begin{bmatrix}-\ddot{w}+U_\infty\cdot\left(\dot{\bar{\alpha}}\cdot\cos\left(\Lambda\right)-\dot{w}'\cdot\sin\left(\Lambda\right)\right)\\ +\bar{b}\cdot\left(\frac{1}{2}-\bar{a}\right)\cdot\left(\ddot{\bar{\alpha}}+U_\infty\cdot\dot{\bar{\alpha}}'\cdot\sin\left(\Lambda\right)\right)\end{bmatrix}\cdot d\tau = \\
& F_{w\alpha\alpha}\cdot\left(1-2\cdot d\right) - F_{w\alpha\alpha}\left(0\right)\cdot\left(1-d\cdot e^{-\kappa_1\cdot t}-d\cdot e^{-\kappa_2\cdot t}\right) \\
& +F_{w\alpha}\cdot d\cdot\left(\kappa_1+\kappa_2\right) - F_{w\alpha}\left(0\right)\cdot d\cdot\left(\kappa_1\cdot e^{-\kappa_1\cdot t}+\kappa_2\cdot e^{-\kappa_2\cdot t}\right) \\
& -\kappa_1^2\cdot d\cdot e^{-\kappa_1\cdot t}\cdot\int_0^t e^{\kappa_1\cdot\tau}\cdot\left[F_{w\alpha}\right]\cdot d\tau + \kappa_1\cdot d\cdot e^{-\kappa_1\cdot t}\cdot\int_0^t e^{\kappa_1\cdot\tau}\cdot\left[U_\infty\cdot\bar{\alpha}\cdot\cos\left(\Lambda\right)\right]\cdot d\tau \\
& -\kappa_1\cdot d\cdot e^{-\kappa_1\cdot t}\cdot\int_0^t e^{\kappa_1\cdot\tau}\cdot\left[U_\infty\cdot w'\cdot\sin\left(\Lambda\right)\right]\cdot d\tau \\
& +\kappa_1\cdot d\cdot e^{-\kappa_1\cdot t}\cdot\int_0^t e^{\kappa_1\cdot\tau}\cdot\bar{b}\cdot\left(\frac{1}{2}-\bar{a}\right)\cdot U_\infty\cdot\bar{\alpha}'\cdot\sin\left(\Lambda\right)\cdot d\tau \\
& -\kappa_2^2\cdot d\cdot e^{-\kappa_2\cdot t}\cdot\int_0^t e^{\kappa_2\cdot\tau}\cdot\left[F_{w\alpha}\right]\cdot d\tau + \kappa_2\cdot d\cdot e^{-\kappa_2\cdot t}\cdot\int_0^t e^{\kappa_2\cdot\tau}\cdot\left[U_\infty\cdot\bar{\alpha}\cdot\cos\left(\Lambda\right)\right]\cdot d\tau \\
& -\kappa_2\cdot d\cdot e^{-\kappa_2\cdot t}\cdot\int_0^t e^{\kappa_2\cdot\tau}\cdot\left[U_\infty\cdot w'\cdot\sin\left(\Lambda\right)\right]\cdot d\tau \\
& +\kappa_2\cdot d\cdot e^{-\kappa_2\cdot t}\cdot\int_0^t e^{\kappa_2\cdot\tau}\cdot\bar{b}\cdot\left(\frac{1}{2}-\bar{a}\right)\cdot U_\infty\cdot\bar{\alpha}'\cdot\sin\left(\Lambda\right)\cdot d\tau
\end{aligned}
\tag{26}
$$

By inserting Eq. (26) into Eq. (20), removing the similar expressions, and simplifying, the lift force and aerodynamic moment of the wing are rewritten as follows.

$$\bar{L} = \pi \cdot \rho_\infty \cdot \bar{b}^2 \cdot \left[-\ddot{w} + U_\infty \cdot \dot{\bar{\alpha}} \cdot \cos(\Lambda) - U_\infty \cdot \dot{w}' \cdot \sin(\Lambda) - \bar{b} \cdot \bar{a} \cdot \ddot{\bar{\alpha}} - \bar{b} \cdot \bar{a} \cdot U_\infty \cdot \dot{\bar{\alpha}}' \cdot \sin(\Lambda) \right]$$

$$+2 \cdot \pi \cdot \rho_\infty \cdot U_\infty \cdot \cos(\Lambda) \cdot \bar{b} \cdot \left\{ \begin{array}{l} \psi(0) \cdot \left[\begin{array}{l} -\dot{w} + U_\infty \cdot \left(\bar{\alpha} \cdot \cos(\Lambda) - w' \cdot \sin(\Lambda) \right) \\ +\bar{b} \cdot \left(\frac{1}{2} - \bar{a} \right) \cdot \left(\dot{\bar{\alpha}} + U_\infty \cdot \bar{\alpha}' \cdot \sin(\Lambda) \right) \end{array} \right] \\ +\dot{\psi}(0) \cdot \left[-w + \bar{b} \cdot \left(\frac{1}{2} - \bar{a} \right) \cdot \bar{\alpha} \right] \\ -\dot{\psi}(t) \cdot \left[-w(0) + \bar{b} \cdot \left(\frac{1}{2} - \bar{a} \right) \cdot \bar{\alpha}(0) \right] \\ +\kappa_1 \cdot d \cdot \left[U_\infty \cdot \cos(\Lambda) - \kappa_1 \cdot \bar{b} \cdot \left(\frac{1}{2} - \bar{a} \right) \right] \cdot e^{-\kappa_1 \cdot t} \cdot \int_0^t e^{\kappa_1 \cdot \tau} \bar{\alpha} \cdot d\tau \\ +\kappa_1 \cdot d \cdot \bar{b} \cdot \left(\frac{1}{2} - \bar{a} \right) \cdot U_\infty \cdot \sin(\Lambda) \cdot e^{-\kappa_1 \cdot t} \cdot \int_0^t e^{\kappa_1 \cdot \tau} \cdot \bar{\alpha}' \cdot d\tau \\ -\kappa_1 \cdot d \cdot U_\infty \cdot \sin(\Lambda) \cdot e^{-\kappa_1 \cdot t} \cdot \int_0^t e^{\kappa_1 \cdot \tau} \cdot w' \cdot d\tau \\ +\kappa_1^2 \cdot d \cdot e^{-\kappa_1 \cdot t} \cdot \int_0^t e^{\kappa_1 \cdot \tau} \cdot w \cdot d\tau \\ +\kappa_2 \cdot d \cdot \left[U_\infty \cdot \cos(\Lambda) - \kappa_2 \cdot \bar{b} \cdot \left(\frac{1}{2} - \bar{a} \right) \right] \cdot e^{-\kappa_2 \cdot t} \cdot \int_0^t e^{\kappa_2 \cdot \tau} \cdot \bar{\alpha} \cdot d\tau \\ +\kappa_2 \cdot d \cdot \bar{b} \cdot \left(\frac{1}{2} - \bar{a} \right) \cdot U_\infty \cdot \sin(\Lambda) \cdot e^{-\kappa_2 \cdot t} \cdot \int_0^t e^{\kappa_2 \cdot \tau} \cdot \bar{\alpha}' \cdot d\tau \\ -\kappa_2 \cdot d \cdot U_\infty \cdot \sin(\Lambda) \cdot e^{-\kappa_2 \cdot t} \cdot \int_0^t e^{\kappa_2 \cdot \tau} \cdot w' \cdot d\tau \\ +\kappa_2^2 \cdot d \cdot e^{-\kappa_2 \cdot t} \cdot \int_0^t e^{\kappa_2 \cdot \tau} \cdot w \cdot d\tau \end{array} \right\} \quad (27)$$

$$\bar{M}_{e.a} = -\pi\cdot\rho_\infty\cdot\bar{b}^3\cdot\begin{bmatrix} U_\infty\cdot\left(\frac{1}{2}-\bar{a}\right)\cdot\dot{\bar{\alpha}}\cdot\cos(\Lambda)+\frac{1}{2}\cdot U_\infty^2\cdot\bar{\alpha}'\cdot\cos(\Lambda)\cdot\sin(\Lambda)+\bar{a}\cdot\dot{w} \\ +U_\infty\cdot\bar{a}\cdot\dot{w}'\cdot\sin(\Lambda)+\bar{b}\cdot\left(\frac{1}{8}+\bar{a}^2\right)\cdot\left(\ddot{\bar{\alpha}}+U_\infty\cdot\dot{\bar{\alpha}}'\cdot\sin(\Lambda)\right)\end{bmatrix}$$

$$+2\cdot\pi\cdot\rho_\infty\cdot U_\infty\cdot\cos(\Lambda)\cdot\bar{b}\cdot\bar{e}\cdot\begin{Bmatrix} \psi(0)\cdot\begin{bmatrix}-\dot{w}+U_\infty\cdot\left(\bar{\alpha}\cdot\cos(\Lambda)-w'\cdot\sin(\Lambda)\right)\\ +\bar{b}\cdot\left(\frac{1}{2}-\bar{a}\right)\cdot\left(\dot{\bar{\alpha}}+U_\infty\cdot\bar{\alpha}'\cdot\sin(\Lambda)\right)\end{bmatrix} \\ +\dot{\psi}(0)\cdot\left[-w+\bar{b}\cdot\left(\frac{1}{2}-\bar{a}\right)\cdot\bar{\alpha}\right] \\ -\dot{\psi}(t)\cdot\left[-w(0)+\bar{b}\cdot\left(\frac{1}{2}-\bar{a}\right)\cdot\bar{\alpha}(0)\right] \\ +\kappa_1\cdot d\cdot\left[U_\infty\cdot\cos(\Lambda)-\kappa_1\cdot\bar{b}\cdot\left(\frac{1}{2}-\bar{a}\right)\right]\cdot e^{-\kappa_1\cdot t}\cdot\int_0^t e^{\kappa_1\cdot\tau}\bar{\alpha}\cdot d\tau \\ +\kappa_1\cdot d\cdot\bar{b}\cdot\left(\frac{1}{2}-\bar{a}\right)\cdot U_\infty\cdot\sin(\Lambda)\cdot e^{-\kappa_1\cdot t}\cdot\int_0^t e^{\kappa_1\cdot\tau}\cdot\bar{\alpha}'\cdot d\tau \\ -\kappa_1\cdot d\cdot U_\infty\cdot\sin(\Lambda)\cdot e^{-\kappa_1\cdot t}\cdot\int_0^t e^{\kappa_1\cdot\tau}\cdot w'\cdot d\tau \\ +\kappa_1^2\cdot d\cdot e^{-\kappa_1\cdot t}\cdot\int_0^t e^{\kappa_1\cdot\tau}\cdot w\cdot d\tau \\ +\kappa_2\cdot d\cdot\left[U_\infty\cdot\cos(\Lambda)-\kappa_2\cdot\bar{b}\cdot\left(\frac{1}{2}-\bar{a}\right)\right]\cdot e^{-\kappa_2\cdot t}\cdot \\ \int_0^t e^{\kappa_2\cdot\tau}\cdot\bar{\alpha}\cdot d\tau \\ +\kappa_2\cdot d\cdot\bar{b}\cdot\left(\frac{1}{2}-\bar{a}\right)\cdot U_\infty\cdot\sin(\Lambda)\cdot e^{-\kappa_2\cdot t}\cdot\int_0^t e^{\kappa_2\cdot\tau}\cdot\bar{\alpha}'\cdot d\tau \\ -\kappa_2\cdot d\cdot U_\infty\cdot\sin(\Lambda)\cdot e^{-\kappa_2\cdot t}\cdot\int_0^t e^{\kappa_2\cdot\tau}\cdot w'\cdot d\tau \\ +\kappa_2^2\cdot d\cdot e^{-\kappa_2\cdot t}\cdot\int_0^t e^{\kappa_2\cdot\tau}\cdot w\cdot d\tau \end{Bmatrix} \tag{28}$$

The integral expressions in the lift force and the aerodynamic moment of the wing in Eq. (28) can be considered as new degrees of freedom and are expressed as follows.

$$B_{si}(\bar{y},t) = e^{-\kappa_i\cdot t}\cdot\int_0^t s(\bar{y},\tau)\cdot e^{\kappa_i\cdot\tau}\cdot d\tau,\quad s(\bar{y},t) = w(\bar{y},t)\ \text{ or }\ \bar{\alpha}(\bar{y},t),\quad i=1,2 \tag{29}$$

By taking the derivative of Eq. (29), the following expression can be written.

$$\begin{aligned}\dot{B}_{si}\left(\bar{y},t\right)&=-\kappa_i\cdot e^{-\kappa_i\cdot t}\cdot\int_0^t s\left(\bar{y},\tau\right)\cdot e^{\kappa_i\cdot\tau}\cdot d\tau+e^{-\kappa_i\cdot t}\cdot s\left(\bar{y},t\right)\cdot e^{\kappa_i\cdot t}\\&=-\kappa_i\cdot B_{si}\left(\bar{y},t\right)+s\left(\bar{y},t\right)\end{aligned}\tag{30}$$

Therefore, the differential equations governing these degrees of freedom are obtained as follows.

$$\begin{aligned}&\dot{B}_{w1}+\varepsilon_1\cdot B_{w1}=w\left(\bar{y},t\right)\\&\dot{B}_{w2}+\varepsilon_2\cdot B_{w2}=w\left(\bar{y},t\right)\\&\dot{B}_{\bar{\alpha}1}+\varepsilon_1\cdot B_{\bar{\alpha}1}=\bar{\alpha}\left(\bar{y},t\right)\\&\dot{B}_{\bar{\alpha}2}+\varepsilon_2\cdot B_{\bar{\alpha}2}=\bar{\alpha}\left(\bar{y},t\right)\end{aligned}\tag{31}$$

For the degrees of freedom in Eq. (31), the mode shapes and the following generalized coordinates can be considered.

$$\begin{aligned}&B_{w1}\left(\bar{y},t\right)=\left\langle\Psi\right\rangle\cdot\left\{r_{w1}\right\}\\&B_{w2}\left(\bar{y},t\right)=\left\langle\Psi\right\rangle\cdot\left\{r_{w2}\right\}\\&B_{\bar{\alpha}1}\left(\bar{y},t\right)=\left\langle\Theta\right\rangle\cdot\left\{r_{\bar{\alpha}1}\right\}\\&B_{\bar{\alpha}2}\left(\bar{y},t\right)=\left\langle\Theta\right\rangle\cdot\left\{r_{\bar{\alpha}2}\right\}\end{aligned}\tag{32}$$

By multiplying the mode shapes in Eq. (31) and integrating, the following conclusion can be reached.

$$\begin{aligned}&\int_0^l\left(\left\{\Psi\right\}\cdot\left\langle\Psi\right\rangle\cdot\left\{\dot{r}_{w1}\right\}+\varepsilon_1\cdot\left\{\Psi\right\}\cdot\left\langle\Psi\right\rangle\cdot\left\{r_{w1}\right\}-\left\{\Psi\right\}\cdot\left\langle\Psi\right\rangle\cdot\left\{r_w\right\}\right)\cdot d\bar{y}=0\\&\int_0^l\left(\left\{\Psi\right\}\cdot\left\langle\Psi\right\rangle\cdot\left\{\dot{r}_{w2}\right\}+\varepsilon_2\cdot\left\{\Psi\right\}\cdot\left\langle\Psi\right\rangle\cdot\left\{r_{w2}\right\}-\left\{\Psi\right\}\cdot\left\langle\Psi\right\rangle\cdot\left\{r_w\right\}\right)\cdot d\bar{y}=0\\&\int_0^l\left(\left\{\Theta\right\}\cdot\left\langle\Theta\right\rangle\cdot\left\{\dot{r}_{\bar{\alpha}1}\right\}+\varepsilon_1\cdot\left\{\Theta\right\}\cdot\left\langle\Theta\right\rangle\cdot\left\{r_{\bar{\alpha}1}\right\}-\left\{\Theta\right\}\cdot\left\langle\Theta\right\rangle\cdot\left\{r_{\bar{\alpha}}\right\}\right)\cdot d\bar{y}=0\\&\int_0^l\left(\left\{\Theta\right\}\cdot\left\langle\Theta\right\rangle\cdot\left\{\dot{r}_{\bar{\alpha}2}\right\}+\varepsilon_2\cdot\left\{\Theta\right\}\cdot\left\langle\Theta\right\rangle\cdot\left\{r_{\bar{\alpha}2}\right\}-\left\{\Theta\right\}\cdot\left\langle\Theta\right\rangle\cdot\left\{r_{\bar{\alpha}}\right\}\right)\cdot d\bar{y}=0\end{aligned}\tag{33}$$

4- Aeroelastic analysis

The structure's equation of motion can be formulated into the following matrix representation, incorporating the lift force and aerodynamic moment according to Eq. (27) and (28) and accounting for the four equations delineated in Eq. (33).

$$\left[M^S-M^A\right]\cdot\left\{\ddot{q}\right\}+\left[C^S-C^A\right]\cdot\left\{\dot{q}\right\}+\left[K^S-K^A\right]\cdot\left\{q\right\}-\left[P\right]\cdot\left\{q\left(0\right)\right\}=\left\{0\right\}\tag{34}$$

Here, M represents the mass matrix, C signifies the damping matrix, K denotes the stiffness matrix, S and A represent the structural and aerodynamic indices of the matrices, respectively, and q

signifies the generalized coordinate matrix. Each of these matrices is derived as described below. The arrays that are not included are equal to zero.

$$\left[M_{11}^{S}\right]=\int_{0}^{l_1}\bar{m}_1\cdot\left\{\Psi_1\right\}\cdot\left\langle\Psi_1\right\rangle\cdot d\bar{y}_1+\int_{0}^{l_2}\bar{m}_2\cdot\left\{\Psi_2\right\}\cdot\left\langle\Psi_2\right\rangle\cdot d\bar{y}_2 \tag{35}$$

$$\left[M_{12}^{S}\right]=-\int_{0}^{l_1}\bar{m}_1\cdot\bar{b}_1\cdot\bar{x}_{\alpha_1}\cdot\left\{\Psi_1\right\}\cdot\left\langle\Theta_1\right\rangle\cdot d\bar{y}_1-\int_{0}^{l_2}\bar{m}_2\cdot\bar{b}_2\cdot\bar{x}_{\alpha_2}\cdot\left\{\Psi_2\right\}\cdot\left\langle\Theta_2\right\rangle\cdot d\bar{y}_2 \tag{36}$$

$$\left[M_{21}^{S}\right]=-\int_{0}^{l_1}\bar{m}_1\cdot\bar{b}_1\cdot\bar{x}_{\alpha_1}\cdot\left\{\Theta_1\right\}\cdot\left\langle\Psi_1\right\rangle\cdot d\bar{y}_1-\int_{0}^{l_2}\bar{m}_2\cdot\bar{b}_2\cdot\bar{x}_{\alpha_2}\cdot\left\{\Theta_2\right\}\cdot\left\langle\Psi_2\right\rangle\cdot d\bar{y}_2 \tag{37}$$

$$\left[M_{22}^{S}\right]=\int_{0}^{l_1}\bar{I}_{\alpha_1}\cdot\left\{\Theta_1\right\}\cdot\left\langle\Theta_1\right\rangle\cdot d\bar{y}_1+\int_{0}^{l_2}\bar{I}_{\alpha_2}\cdot\left\{\Theta_2\right\}\cdot\left\langle\Theta_2\right\rangle\cdot d\bar{y}_2 \tag{38}$$

$$\left[K_{11}^{S}\right]=\int_{0}^{l_1}\overline{EI}_1\cdot\left\{\Psi_1''\right\}\cdot\left\langle\Psi_1''\right\rangle\cdot d\bar{y}_1+\int_{0}^{l_2}\overline{EI}_2\cdot\left\{\Psi_2''\right\}\cdot\left\langle\Psi_2''\right\rangle\cdot d\bar{y}_2 \tag{39}$$

$$\left[K_{22}^{S}\right]=\int_{0}^{l_1}\overline{GJ}_1\cdot\left\{\Theta_1'\right\}\cdot\left\langle\Theta_1'\right\rangle\cdot d\bar{y}_1+\int_{0}^{l_2}\overline{GJ}_2\cdot\left\{\Theta_2'\right\}\cdot\left\langle\Theta_2'\right\rangle\cdot d\bar{y}_2 \tag{40}$$

$$\left[M_{11}^{A}\right]=-\int_{0}^{l_1}\pi\cdot\rho_\infty\cdot\bar{b}_1^{2}\cdot\left\{\Psi_1\right\}\cdot\left\langle\Psi_1\right\rangle\cdot d\bar{y}_1-\int_{0}^{l_2}\pi\cdot\rho_\infty\cdot\bar{b}_2^{2}\cdot\left\{\Psi_2\right\}\cdot\left\langle\Psi_2\right\rangle\cdot d\bar{y}_2 \tag{41}$$

$$\left[M_{12}^{A}\right]=-\int_{0}^{l_1}\pi\cdot\rho_\infty\cdot\bar{b}_1^{3}\cdot\bar{a}_1\cdot\left\{\Psi_1\right\}\cdot\left\langle\Theta_1\right\rangle\cdot d\bar{y}_1-\int_{0}^{l_2}\pi\cdot\rho_\infty\cdot\bar{b}_2^{3}\cdot\bar{a}_2\cdot\left\{\Psi_2\right\}\cdot\left\langle\Theta_2\right\rangle\cdot d\bar{y}_2 \tag{42}$$

$$\left[M_{21}^{A}\right]=-\int_{0}^{l_1}\pi\cdot\rho_\infty\cdot\bar{b}_1^{3}\cdot\bar{a}_1\cdot\left\{\Theta_1\right\}\cdot\left\langle\Psi_1\right\rangle\cdot d\bar{y}_1-\int_{0}^{l_2}\pi\cdot\rho_\infty\cdot\bar{b}_2^{3}\cdot\bar{a}_2\cdot\left\{\Theta_2\right\}\cdot\left\langle\Psi_2\right\rangle\cdot d\bar{y}_2 \tag{43}$$

$$\left[M_{22}^{A}\right]=\begin{Bmatrix}-\int_{0}^{l_1}\pi\cdot\rho_\infty\cdot\bar{b}_1^{4}\cdot\left(\frac{1}{8}+\bar{a}_1^{2}\right)\cdot\left\{\Theta_1\right\}\cdot\left\langle\Theta_1\right\rangle\cdot d\bar{y}_1\\ -\int_{0}^{l_2}\pi\cdot\rho_\infty\cdot\bar{b}_2^{4}\cdot\left(\frac{1}{8}+\bar{a}_2^{2}\right)\cdot\left\{\Theta_2\right\}\cdot\left\langle\Theta_2\right\rangle\cdot d\bar{y}_2\end{Bmatrix} \tag{44}$$

$$\left[C_{11}^{A}\right]=\begin{Bmatrix}-\int_{0}^{l_1}\pi\cdot\rho_\infty\cdot U_\infty\cdot\cos\left(\theta-\Lambda_1\right)\cdot\bar{b}_1^{2}\cdot\left\{\Psi_1\right\}\cdot\left\langle\Psi_1'\right\rangle\cdot d\bar{y}_1\\ -\int_{0}^{l_1}2\cdot\pi\cdot\rho_\infty\cdot U_\infty\cdot\sin\left(\theta-\Lambda_1\right)\cdot\psi\left(0\right)\cdot\bar{b}_1\cdot\left\{\Psi_1\right\}\cdot\left\langle\Psi_1\right\rangle\cdot d\bar{y}_1\\ -\int_{0}^{l_2}\pi\cdot\rho_\infty\cdot U_\infty\cdot\cos\left(\theta-\Lambda_2\right)\cdot\bar{b}_2^{2}\cdot\left\{\Psi_2\right\}\cdot\left\langle\Psi_2'\right\rangle\cdot d\bar{y}_2\\ -\int_{0}^{l_2}2\cdot\pi\cdot\rho_\infty\cdot U_\infty\cdot\sin\left(\theta-\Lambda_2\right)\cdot\psi\left(0\right)\cdot\bar{b}_2\cdot\left\{\Psi_2\right\}\cdot\left\langle\Psi_2\right\rangle\cdot d\bar{y}_2\end{Bmatrix} \tag{45}$$

$$\left[C_{12}^{A}\right]=\begin{Bmatrix}\int_0^{l_1}\pi\cdot\rho_\infty\cdot U_\infty\cdot\bar{b}_1^{\,2}\cdot\begin{pmatrix}\sin\left(\theta-\Lambda_1\right)\cdot\left\{\Psi_1\right\}\cdot\left\langle\Theta_1\right\rangle\\-\cos\left(\theta-\Lambda_1\right)\cdot\bar{b}_1\cdot\bar{a}_1\cdot\left\{\Psi_1\right\}\cdot\left\langle\Theta_1'\right\rangle\end{pmatrix}\cdot d\bar{y}_1\\+\int_0^{l_1}2\cdot\pi\cdot\rho_\infty\cdot U_\infty\cdot\sin\left(\theta-\Lambda_1\right)\cdot\psi\left(0\right)\cdot\bar{b}_1^{\,2}\cdot\left(\frac{1}{2}-\bar{a}_1\right)\cdot\left\{\Psi_1\right\}\cdot\left\langle\Theta_1\right\rangle\cdot d\bar{y}_1\\\int_0^{l_2}\pi\cdot\rho_\infty\cdot U_\infty\cdot\bar{b}_2^{\,2}\cdot\begin{pmatrix}\sin\left(\theta-\Lambda_2\right)\cdot\left\{\Psi_2\right\}\cdot\left\langle\Theta_2\right\rangle\\-\cos\left(\theta-\Lambda_2\right)\cdot\bar{b}_2\cdot\bar{a}_2\cdot\left\{\Psi_2\right\}\cdot\left\langle\Theta_2'\right\rangle\end{pmatrix}\cdot d\bar{y}_2\\+\int_0^{l_2}2\cdot\pi\cdot\rho_\infty\cdot U_\infty\cdot\sin\left(\theta-\Lambda_2\right)\cdot\psi\left(0\right)\cdot\bar{b}_2^{\,2}\cdot\left(\frac{1}{2}-\bar{a}_2\right)\cdot\left\{\Psi_2\right\}\cdot\left\langle\Theta_2\right\rangle\cdot d\bar{y}_2\end{Bmatrix} \tag{46}$$

$$\left[C_{21}^{A}\right]=\begin{Bmatrix}-\int_0^{l_1}\pi\cdot\rho_\infty\cdot U_\infty\cdot\cos\left(\theta-\Lambda_1\right)\cdot\bar{b}_1^{\,3}\cdot\bar{a}_1\cdot\left\{\Theta_1\right\}\cdot\left\langle\Psi_1'\right\rangle\cdot d\bar{y}_1\\-\int_0^{l_1}2\cdot\pi\cdot\rho_\infty\cdot U_\infty\cdot\sin\left(\theta-\Lambda_1\right)\cdot\psi\left(0\right)\cdot\bar{b}_1\cdot\bar{e}_1\cdot\left\{\Theta_1\right\}\cdot\left\langle\Psi_1\right\rangle\cdot d\bar{y}_1\\-\int_0^{l_2}\pi\cdot\rho_\infty\cdot U_\infty\cdot\cos\left(\theta-\Lambda_2\right)\cdot\bar{b}_2^{\,3}\cdot\bar{a}_2\cdot\left\{\Theta_2\right\}\cdot\left\langle\Psi_2'\right\rangle\cdot d\bar{y}_2\\-\int_0^{l_2}2\cdot\pi\cdot\rho_\infty\cdot U_\infty\cdot\sin\left(\theta-\Lambda_2\right)\cdot\psi\left(0\right)\cdot\bar{b}_2\cdot\bar{e}_2\cdot\left\{\Theta_2\right\}\cdot\left\langle\Psi_2\right\rangle\cdot d\bar{y}_2\end{Bmatrix} \tag{47}$$

$$\left[C_{22}^{A}\right]=\begin{Bmatrix}-\int_0^{l_1}\pi\cdot\rho_\infty\cdot U_\infty\cdot\bar{b}_1^{\,3}\cdot\begin{bmatrix}\sin\left(\theta-\Lambda_1\right)\cdot\left(\frac{1}{2}-\bar{a}_1\right)\cdot\left\{\Theta_1\right\}\cdot\left\langle\Theta_1\right\rangle\\+\cos\left(\theta-\Lambda_1\right)\cdot\bar{b}_1\cdot\left(\frac{1}{8}+\bar{a}_1^{\,2}\right)\cdot\left\{\Theta_1\right\}\cdot\left\langle\Theta_1'\right\rangle\end{bmatrix}\cdot d\bar{y}_1\\+\int_0^{l_1}2\cdot\pi\cdot\rho_\infty\cdot U_\infty\cdot\sin\left(\theta-\Lambda_1\right)\cdot\psi\left(0\right)\cdot\bar{b}_1^{\,2}\cdot\bar{e}_1\cdot\left(\frac{1}{2}-\bar{a}_1\right)\cdot\left\{\Theta_1\right\}\cdot\left\langle\Theta_1\right\rangle\cdot d\bar{y}_1\\-\int_0^{l_2}\pi\cdot\rho_\infty\cdot U_\infty\cdot\bar{b}_2^{\,3}\cdot\begin{bmatrix}\sin\left(\theta-\Lambda_2\right)\cdot\left(\frac{1}{2}-\bar{a}_2\right)\cdot\left\{\Theta_2\right\}\cdot\left\langle\Theta_2\right\rangle\\+\cos\left(\theta-\Lambda_2\right)\cdot\bar{b}_2\cdot\left(\frac{1}{8}+\bar{a}_2^{\,2}\right)\cdot\left\{\Theta_2\right\}\cdot\left\langle\Theta_2'\right\rangle\end{bmatrix}\cdot d\bar{y}_2\\+\int_0^{l_2}2\cdot\pi\cdot\rho_\infty\cdot U_\infty\cdot\sin\left(\theta-\Lambda_2\right)\cdot\psi\left(0\right)\cdot\bar{b}_2^{\,2}\cdot\bar{e}_2\cdot\left(\frac{1}{2}-\bar{a}_2\right)\cdot\left\{\Theta_2\right\}\cdot\left\langle\Theta_2\right\rangle\cdot d\bar{y}_2\end{Bmatrix} \tag{48}$$

$$\left[C_{33}^{A}\right]=-\int_0^{l_1}\left\{\Psi_1\right\}\cdot\left\langle\Psi_1\right\rangle\cdot d\bar{y}_1-\int_0^{l_2}\left\{\Psi_2\right\}\cdot\left\langle\Psi_2\right\rangle\cdot d\bar{y}_2 \tag{49}$$

$$\left[C_{44}^{A}\right]=-\int_0^{l_1}\left\{\Psi_1\right\}\cdot\left\langle\Psi_1\right\rangle\cdot d\bar{y}_1-\int_0^{l_2}\left\{\Psi_2\right\}\cdot\left\langle\Psi_2\right\rangle\cdot d\bar{y}_2 \tag{50}$$

$$\left[C_{55}^{A}\right]=-\int_{0}^{l_1}\left\{\Theta_1\right\}\cdot\left\langle\Theta_1\right\rangle\cdot d\bar{y}_1-\int_{0}^{l_2}\left\{\Theta_2\right\}\cdot\left\langle\Theta_2\right\rangle\cdot d\bar{y}_2 \tag{51}$$

$$\left[C_{66}^{A}\right]=-\int_{0}^{l_1}\left\{\Theta_1\right\}\cdot\left\langle\Theta_1\right\rangle\cdot d\bar{y}_1-\int_{0}^{l_2}\left\{\Theta_2\right\}\cdot\left\langle\Theta_2\right\rangle\cdot d\bar{y}_2 \tag{52}$$

$$\left[K_{11}^{A}\right]=\begin{Bmatrix}-\int_{0}^{l_1}2\cdot\pi\cdot\rho_\infty\cdot U_\infty\cdot\sin\left(\theta-\Lambda_1\right)\cdot\bar{b}_1\cdot\begin{bmatrix}U_\infty\cdot\cos\left(\theta-\Lambda_1\right)\cdot\psi\left(0\right)\cdot\left\{\Psi_1\right\}\cdot\left\langle\Psi_1'\right\rangle\\+\dot{\psi}\left(0\right)\cdot\left\{\Psi_1\right\}\cdot\left\langle\Psi_1\right\rangle\end{bmatrix}\cdot d\bar{y}_1\\-\int_{0}^{l_2}2\cdot\pi\cdot\rho_\infty\cdot U_\infty\cdot\sin\left(\theta-\Lambda_2\right)\cdot\bar{b}_2\cdot\begin{bmatrix}U_\infty\cdot\cos\left(\theta-\Lambda_2\right)\cdot\psi\left(0\right)\cdot\left\{\Psi_2\right\}\cdot\left\langle\Psi_2'\right\rangle\\+\dot{\psi}\left(0\right)\cdot\left\{\Psi_2\right\}\cdot\left\langle\Psi_2\right\rangle\end{bmatrix}\cdot d\bar{y}_2\end{Bmatrix} \tag{53}$$

$$\left[K_{12}^{A}\right]=\begin{Bmatrix}\int_{0}^{l_1}2\cdot\pi\cdot\rho_\infty\cdot U_\infty\cdot\sin\left(\theta-\Lambda_1\right)\cdot\bar{b}_1\cdot\begin{bmatrix}U_\infty\cdot\psi\left(0\right)\cdot\begin{pmatrix}\sin\left(\theta-\Lambda_1\right)\cdot\left\{\Psi_1\right\}\cdot\left\langle\Theta_1\right\rangle\\+\cos\left(\theta-\Lambda_1\right)\cdot\\\bar{b}_1\cdot\left(\frac{1}{2}-\bar{a}_1\right)\cdot\left\{\Psi_1\right\}\cdot\left\langle\Theta_1'\right\rangle\end{pmatrix}\\+\dot{\psi}\left(0\right)\cdot\bar{b}_1\cdot\left(\frac{1}{2}-\bar{a}_1\right)\cdot\left\{\Psi_1\right\}\cdot\left\langle\Theta_1\right\rangle\end{bmatrix}\cdot d\bar{y}_1\\+\int_{0}^{l_2}2\cdot\pi\cdot\rho_\infty\cdot U_\infty\cdot\sin\left(\theta-\Lambda_2\right)\cdot\bar{b}_2\cdot\begin{bmatrix}U_\infty\cdot\psi\left(0\right)\cdot\begin{pmatrix}\sin\left(\theta-\Lambda_2\right)\cdot\left\{\Psi_2\right\}\cdot\left\langle\Theta_2\right\rangle\\+\cos\left(\theta-\Lambda_2\right)\cdot\\\bar{b}_2\cdot\left(\frac{1}{2}-\bar{a}_2\right)\cdot\left\{\Psi_2\right\}\cdot\left\langle\Theta_2'\right\rangle\end{pmatrix}\\+\dot{\psi}\left(0\right)\cdot\bar{b}_2\cdot\left(\frac{1}{2}-\bar{a}_2\right)\cdot\left\{\Psi_2\right\}\cdot\left\langle\Theta_2\right\rangle\end{bmatrix}\cdot d\bar{y}_2\end{Bmatrix} \tag{54}$$

$$\left[K_{13}^{A}\right]=\begin{Bmatrix}\int_{0}^{l_1}2\cdot\pi\cdot\rho_\infty\cdot U_\infty\cdot\sin\left(\theta-\Lambda_1\right)\cdot\bar{b}_1\cdot\kappa_1\cdot d\cdot\begin{pmatrix}\kappa_1\cdot\left\{\Psi_1\right\}\cdot\left\langle\Psi_1\right\rangle\\-U_\infty\cdot\cos\left(\theta-\Lambda_1\right)\cdot\left\{\Psi_1\right\}\cdot\left\langle\Psi_1'\right\rangle\end{pmatrix}\cdot d\bar{y}_1\\+\int_{0}^{l_2}2\cdot\pi\cdot\rho_\infty\cdot U_\infty\cdot\sin\left(\theta-\Lambda_2\right)\cdot\bar{b}_2\cdot\kappa_1\cdot d\cdot\begin{pmatrix}\kappa_1\cdot\left\{\Psi_2\right\}\cdot\left\langle\Psi_2\right\rangle\\-U_\infty\cdot\cos\left(\theta-\Lambda_2\right)\cdot\left\{\Psi_2\right\}\cdot\left\langle\Psi_2'\right\rangle\end{pmatrix}\cdot d\bar{y}_2\end{Bmatrix} \tag{55}$$

$$\left[K_{14}^{A}\right]=\begin{Bmatrix}\int_{0}^{l_1}2\cdot\pi\cdot\rho_\infty\cdot U_\infty\cdot\sin\left(\theta-\Lambda_1\right)\cdot\bar{b}_1\cdot\kappa_2\cdot d\cdot\begin{pmatrix}\kappa_2\cdot\left\{\Psi_1\right\}\cdot\left\langle\Psi_1\right\rangle\\-U_\infty\cdot\cos\left(\theta-\Lambda_1\right)\cdot\left\{\Psi_1\right\}\cdot\left\langle\Psi_1'\right\rangle\end{pmatrix}\cdot d\bar{y}_1\\+\int_{0}^{l_2}2\cdot\pi\cdot\rho_\infty\cdot U_\infty\cdot\sin\left(\theta-\Lambda_2\right)\cdot\bar{b}_2\cdot\kappa_2\cdot d\cdot\begin{pmatrix}\kappa_2\cdot\left\{\Psi_2\right\}\cdot\left\langle\Psi_2\right\rangle\\-U_\infty\cdot\cos\left(\theta-\Lambda_2\right)\cdot\left\{\Psi_2\right\}\cdot\left\langle\Psi_2'\right\rangle\end{pmatrix}\cdot d\bar{y}_2\end{Bmatrix} \tag{56}$$

$$\left[K_{15}^{A}\right]=\left\{\int_{0}^{l_1}2\cdot\pi\cdot\rho_{\infty}\cdot U_{\infty}\cdot\sin\left(\theta-\Lambda_1\right)\cdot\bar{b}_1\cdot\kappa_1\cdot d\cdot\begin{bmatrix}\left(U_{\infty}\cdot\sin\left(\theta-\Lambda_1\right)\right)\\\left(-\kappa_1\cdot\bar{b}_1\cdot\left(\frac{1}{2}-\bar{a}_1\right)\right)\end{bmatrix}\cdot\left\{\Psi_1\right\}\cdot\left\langle\Theta_1\right\rangle\right.$$
$$\left.\begin{bmatrix}+U_{\infty}\cdot\cos\left(\theta-\Lambda_1\right)\cdot\\\bar{b}_1\cdot\left(\frac{1}{2}-\bar{a}_1\right)\cdot\left\{\Psi_1\right\}\cdot\left\langle\Theta_1'\right\rangle\end{bmatrix}\cdot d\bar{y}_1\right.$$
$$\left.+\int_{0}^{l_2}2\cdot\pi\cdot\rho_{\infty}\cdot U_{\infty}\cdot\sin\left(\theta-\Lambda_2\right)\cdot\bar{b}_2\cdot\kappa_1\cdot d\cdot\begin{bmatrix}\left(U_{\infty}\cdot\sin\left(\theta-\Lambda_2\right)\right)\\\left(-\kappa_1\cdot\bar{b}_2\cdot\left(\frac{1}{2}-\bar{a}_2\right)\right)\end{bmatrix}\cdot\left\{\Psi_2\right\}\cdot\left\langle\Theta_2\right\rangle\right.$$
$$\left.\begin{bmatrix}+U_{\infty}\cdot\cos\left(\theta-\Lambda_2\right)\cdot\\\bar{b}_2\cdot\left(\frac{1}{2}-\bar{a}_2\right)\cdot\left\{\Psi_2\right\}\cdot\left\langle\Theta_2'\right\rangle\end{bmatrix}\cdot d\bar{y}_2\right\}\tag{57}$$

$$\left[K_{16}^{A}\right]=\left\{\int_{0}^{l_1}2\cdot\pi\cdot\rho_{\infty}\cdot U_{\infty}\cdot\sin\left(\theta-\Lambda_1\right)\cdot\bar{b}_1\cdot\kappa_2\cdot d\cdot\begin{bmatrix}\left(U_{\infty}\cdot\sin\left(\theta-\Lambda_1\right)\right)\\\left(-\kappa_2\cdot\bar{b}_1\cdot\left(\frac{1}{2}-\bar{a}_1\right)\right)\end{bmatrix}\cdot\left\{\Psi_1\right\}\cdot\left\langle\Theta_1\right\rangle\right.$$
$$\left.\begin{bmatrix}+\bar{b}_1\cdot\left(\frac{1}{2}-\bar{a}_1\right)\cdot\\U_{\infty}\cdot\cos\left(\theta-\Lambda_1\right)\cdot\left\{\Psi_1\right\}\cdot\left\langle\Theta_1'\right\rangle\end{bmatrix}\cdot d\bar{y}_1+\right.$$
$$\left.\int_{0}^{l_2}2\cdot\pi\cdot\rho_{\infty}\cdot U_{\infty}\cdot\sin\left(\theta-\Lambda_2\right)\cdot\bar{b}_2\cdot\kappa_2\cdot d\cdot\begin{bmatrix}\left(U_{\infty}\cdot\sin\left(\theta-\Lambda_2\right)\right)\\\left(-\kappa_2\cdot\bar{b}_2\cdot\left(\frac{1}{2}-\bar{a}_2\right)\right)\end{bmatrix}\cdot\left\{\Psi_2\right\}\cdot\left\langle\Theta_2\right\rangle\right.$$
$$\left.\begin{bmatrix}+\bar{b}_2\cdot\left(\frac{1}{2}-\bar{a}_2\right)\cdot\\U_{\infty}\cdot\cos\left(\theta-\Lambda_2\right)\cdot\left\{\Psi_2\right\}\cdot\left\langle\Theta_2'\right\rangle\end{bmatrix}\cdot d\bar{y}_2\right\}\tag{58}$$

$$\left[K_{21}^{A}\right]=\begin{Bmatrix} -\int_{0}^{l_1}\pi\cdot\rho_{\infty}\cdot U_{\infty}^{2}\cdot\sin\left(2\cdot\left(\theta-\Lambda_1\right)\right)\cdot\psi\left(0\right)\cdot\bar{b}_1\cdot\bar{e}_1\cdot\left\{\Theta_1\right\}\cdot\left\langle\Psi'_1\right\rangle\cdot d\bar{y}_1 \\ -\int_{0}^{l_1}2\cdot\pi\cdot\rho_{\infty}\cdot U_{\infty}\cdot\sin\left(\theta-\Lambda_1\right)\cdot\dot{\psi}\left(0\right)\cdot\bar{b}_1\cdot\bar{e}_1\cdot\left\{\Theta_1\right\}\cdot\left\langle\Psi_1\right\rangle\cdot d\bar{y}_1 \\ -\int_{0}^{l_2}\pi\cdot\rho_{\infty}\cdot U_{\infty}^{2}\cdot\sin\left(2\cdot\left(\theta-\Lambda_2\right)\right)\cdot\psi\left(0\right)\cdot\bar{b}_2\cdot\bar{e}_2\cdot\left\{\Theta_2\right\}\cdot\left\langle\Psi'_2\right\rangle\cdot d\bar{y}_2 \\ -\int_{0}^{l_2}2\cdot\pi\cdot\rho_{\infty}\cdot U_{\infty}\cdot\sin\left(\theta-\Lambda_2\right)\cdot\dot{\psi}\left(0\right)\cdot\bar{b}_2\cdot\bar{e}_2\cdot\left\{\Theta_2\right\}\cdot\left\langle\Psi_2\right\rangle\cdot d\bar{y}_2 \end{Bmatrix} \tag{59}$$

$$\left[K_{22}^{A}\right]=\begin{Bmatrix} -\int_{0}^{l_1}\frac{1}{4}\cdot\pi\cdot\rho_{\infty}\cdot U_{\infty}^{2}\cdot\sin\left(2\cdot\left(\theta-\Lambda_1\right)\right)\cdot\bar{b}_1^{3}\cdot\left\{\Theta_1\right\}\cdot\left\langle\Theta'_1\right\rangle\cdot d\bar{y}_1 \\ +\int_{0}^{l_1}2\cdot\pi\cdot\rho_{\infty}\cdot U_{\infty}\cdot\sin\left(\theta-\Lambda_1\right)\cdot\bar{b}_1\cdot\bar{e}_1\cdot\left(\begin{matrix} U_{\infty}\cdot\psi\left(0\right)\cdot\begin{bmatrix}\sin\left(\theta-\Lambda_1\right)\cdot\\ \left\{\Theta_1\right\}\cdot\left\langle\Theta_1\right\rangle\\ +\cos\left(\theta-\Lambda_1\right)\cdot\\ \bar{b}_1\cdot\left(\frac{1}{2}-\bar{a}_1\right)\cdot\\ \left\{\Theta_1\right\}\cdot\left\langle\Theta'_1\right\rangle\end{bmatrix}\\ +\dot{\psi}\left(0\right)\cdot\bar{b}_1\cdot\left(\frac{1}{2}-\bar{a}_1\right)\cdot\left\{\Theta_1\right\}\cdot\left\langle\Theta_1\right\rangle\end{matrix}\right)\cdot d\bar{y}_1 \\ -\int_{0}^{l_2}\frac{1}{4}\cdot\pi\cdot\rho_{\infty}\cdot U_{\infty}^{2}\cdot\sin\left(2\cdot\left(\theta-\Lambda_2\right)\right)\cdot\bar{b}_2^{3}\cdot\left\{\Theta_2\right\}\cdot\left\langle\Theta'_2\right\rangle\cdot d\bar{y}_2 \\ +\int_{0}^{l_2}2\cdot\pi\cdot\rho_{\infty}\cdot U_{\infty}\cdot\sin\left(\theta-\Lambda_2\right)\cdot\bar{b}_2\cdot\bar{e}_2\cdot\left(\begin{matrix} U_{\infty}\cdot\psi\left(0\right)\cdot\begin{bmatrix}\sin\left(\theta-\Lambda_2\right)\cdot\\ \left\{\Theta_2\right\}\cdot\left\langle\Theta_2\right\rangle\\ +\cos\left(\theta-\Lambda_2\right)\cdot\\ \bar{b}_2\cdot\left(\frac{1}{2}-\bar{a}_2\right)\cdot\\ \left\{\Theta_2\right\}\cdot\left\langle\Theta'_2\right\rangle\end{bmatrix}\\ +\dot{\psi}\left(0\right)\cdot\bar{b}_2\cdot\left(\frac{1}{2}-\bar{a}_2\right)\cdot\left\{\Theta_2\right\}\cdot\left\langle\Theta_2\right\rangle\end{matrix}\right)\cdot d\bar{y}_2 \end{Bmatrix} \tag{60}$$

$$\left[K_{23}^{A}\right]=\left\{\begin{array}{l}\int_{0}^{l_1}2\cdot\pi\cdot\rho_{\infty}\cdot U_{\infty}\cdot\sin\left(\theta-\Lambda_1\right)\cdot\kappa_1\cdot d\cdot\bar{b}_1\cdot\bar{e}_1\cdot\left(\begin{array}{l}\kappa_1\cdot\left\{\Theta_1\right\}\cdot\left\langle\Psi_1\right\rangle\\-U_{\infty}\cdot\cos\left(\theta-\Lambda_1\right)\cdot\left\{\Theta_1\right\}\cdot\left\langle\Psi_1'\right\rangle\end{array}\right)\cdot d\bar{y}_1\\+\int_{0}^{l_2}2\cdot\pi\cdot\rho_{\infty}\cdot U_{\infty}\cdot\sin\left(\theta-\Lambda_2\right)\cdot\kappa_1\cdot d\cdot\bar{b}_2\cdot\bar{e}_2\cdot\left(\begin{array}{l}\kappa_1\cdot\left\{\Theta_2\right\}\cdot\left\langle\Psi_2\right\rangle\\-U_{\infty}\cdot\cos\left(\theta-\Lambda_2\right)\cdot\\\left\{\Theta_2\right\}\cdot\left\langle\Psi_2'\right\rangle\end{array}\right)\cdot d\bar{y}_2\end{array}\right\} \tag{61}$$

$$\left[K_{24}^{A}\right]=\left\{\begin{array}{l}\int_{0}^{l_1}2\cdot\pi\cdot\rho_{\infty}\cdot U_{\infty}\cdot\sin\left(\theta-\Lambda_1\right)\cdot\kappa_2\cdot d\cdot\bar{b}_1\cdot\bar{e}_1\cdot\left(\begin{array}{l}\kappa_2\cdot\left\{\Theta_1\right\}\cdot\left\langle\Psi_1\right\rangle\\-U_{\infty}\cdot\cos\left(\theta-\Lambda_1\right)\cdot\left\{\Theta_1\right\}\cdot\left\langle\Psi_1'\right\rangle\end{array}\right)\cdot d\bar{y}_1\\+\int_{0}^{l_2}2\cdot\pi\cdot\rho_{\infty}\cdot U_{\infty}\cdot\sin\left(\theta-\Lambda_2\right)\cdot\kappa_2\cdot d\cdot\bar{b}_2\cdot\bar{e}_2\cdot\left(\begin{array}{l}\kappa_2\cdot\left\{\Theta_2\right\}\cdot\left\langle\Psi_2\right\rangle\\-U_{\infty}\cdot\cos\left(\theta-\Lambda_2\right)\cdot\\\left\{\Theta_2\right\}\cdot\left\langle\Psi_2'\right\rangle\end{array}\right)\cdot d\bar{y}_2\end{array}\right\} \tag{62}$$

$$\left[K_{25}^{A}\right]=\left\{\begin{array}{l}\int_{0}^{l_1}2\cdot\pi\cdot\rho_{\infty}\cdot U_{\infty}\cdot\sin\left(\theta-\Lambda_1\right)\cdot\kappa_1\cdot d\cdot\bar{b}_1\cdot\bar{e}_1\cdot\left[\begin{array}{l}\left(U_{\infty}\cdot\sin\left(\theta-\Lambda_1\right)\right)\\\left(-\kappa_1\cdot\bar{b}_1\cdot\left(\frac{1}{2}-\bar{a}_1\right)\right)\end{array}\right.\cdot\left\{\Theta_1\right\}\cdot\left\langle\Theta_1\right\rangle\\\left.\begin{array}{l}+U_{\infty}\cdot\cos\left(\theta-\Lambda_1\right)\\\cdot\bar{b}_1\cdot\left(\frac{1}{2}-\bar{a}_1\right)\cdot\left\{\Theta_1\right\}\cdot\left\langle\Theta_1'\right\rangle\end{array}\right]\cdot d\bar{y}_1\\+\int_{0}^{l_2}2\cdot\pi\cdot\rho_{\infty}\cdot U_{\infty}\cdot\sin\left(\theta-\Lambda_2\right)\cdot\kappa_1\cdot d\cdot\bar{b}_2\cdot\bar{e}_2\cdot\left[\begin{array}{l}\left(U_{\infty}\cdot\sin\left(\theta-\Lambda_2\right)\right)\\\left(-\kappa_1\cdot\bar{b}_2\cdot\left(\frac{1}{2}-\bar{a}_2\right)\right)\cdot\\\left\{\Theta_2\right\}\cdot\left\langle\Theta_2\right\rangle\\+U_{\infty}\cdot\cos\left(\theta-\Lambda_2\right)\\\cdot\bar{b}_2\cdot\left(\frac{1}{2}-\bar{a}_2\right)\cdot\left\{\Theta_2\right\}\cdot\left\langle\Theta_2'\right\rangle\end{array}\right]\cdot d\bar{y}_2\end{array}\right\} \tag{63}$$

$$\left[K_{26}^{A}\right]=\left\{\begin{array}{l}\int_{0}^{l_1}2\cdot\pi\cdot\rho_{\infty}\cdot U_{\infty}\cdot\sin\left(\theta-\Lambda_1\right)\cdot\kappa_2\cdot d\cdot\bar{b}_1\cdot\bar{e}_1\cdot\left[\begin{array}{l}\left(\begin{array}{l}U_{\infty}\cdot\sin\left(\theta-\Lambda_1\right)\\-\kappa_2\cdot\bar{b}_1\cdot\left(\frac{1}{2}-\bar{a}_1\right)\end{array}\right)\cdot\left\{\Theta_1\right\}\cdot\left\langle\Theta_1\right\rangle\\+\bar{b}_1\cdot\left(\frac{1}{2}-\bar{a}_1\right)\\\cdot U_{\infty}\cdot\cos\left(\theta-\Lambda_1\right)\cdot\left\{\Theta_1\right\}\cdot\left\langle\Theta_1'\right\rangle\end{array}\right]\cdot d\bar{y}_1\\\int_{0}^{l_2}2\cdot\pi\cdot\rho_{\infty}\cdot U_{\infty}\cdot\sin\left(\theta-\Lambda_2\right)\cdot\kappa_2\cdot d\cdot\bar{b}_2\cdot\bar{e}_2\cdot\left[\begin{array}{l}\left(\begin{array}{l}U_{\infty}\cdot\sin\left(\theta-\Lambda_2\right)\\-\kappa_2\cdot\bar{b}_2\cdot\left(\frac{1}{2}-\bar{a}_2\right)\end{array}\right)\cdot\\\left\{\Theta_2\right\}\cdot\left\langle\Theta_2\right\rangle\\+\bar{b}_2\cdot\left(\frac{1}{2}-\bar{a}_2\right)\\\cdot U_{\infty}\cdot\cos\left(\theta-\Lambda_2\right)\cdot\left\{\Theta_2\right\}\cdot\left\langle\Theta_2'\right\rangle\end{array}\right]\cdot d\bar{y}_2\end{array}\right\} \tag{64}$$

$$\left[K_{31}^{A}\right]=\int_{0}^{l_1}\left\{\Psi_1\right\}\cdot\left\langle\Psi_1\right\rangle\cdot d\bar{y}_1+\int_{0}^{l_2}\left\{\Psi_2\right\}\cdot\left\langle\Psi_2\right\rangle\cdot d\bar{y}_2 \tag{65}$$

$$\left[K_{33}^{A}\right]=-\int_{0}^{l_1}\kappa_1\cdot\left\{\Psi_1\right\}\cdot\left\langle\Psi_1\right\rangle\cdot d\bar{y}_1-\int_{0}^{l_2}\kappa_1\cdot\left\{\Psi_2\right\}\cdot\left\langle\Psi_2\right\rangle\cdot d\bar{y}_2 \tag{66}$$

$$\left[K_{41}^{A}\right]=\int_{0}^{l_1}\left\{\Psi_1\right\}\cdot\left\langle\Psi_1\right\rangle\cdot d\bar{y}_1+\int_{0}^{l_2}\left\{\Psi_2\right\}\cdot\left\langle\Psi_2\right\rangle\cdot d\bar{y}_2 \tag{67}$$

$$\left[K_{44}^{A}\right]=-\int_{0}^{l_1}\kappa_2\cdot\left\{\Psi_1\right\}\cdot\left\langle\Psi_1\right\rangle\cdot d\bar{y}_1-\int_{0}^{l_2}\kappa_2\cdot\left\{\Psi_2\right\}\cdot\left\langle\Psi_2\right\rangle\cdot d\bar{y}_2 \tag{68}$$

$$\left[K_{52}^{A}\right]=\int_{0}^{l_1}\left\{\Theta_1\right\}\cdot\left\langle\Theta_1\right\rangle\cdot d\bar{y}_1+\int_{0}^{l_2}\left\{\Theta_2\right\}\cdot\left\langle\Theta_2\right\rangle\cdot d\bar{y}_2 \tag{69}$$

$$\left[K_{55}^{A}\right]=-\int_{0}^{l_1}\kappa_1\cdot\left\{\Theta_1\right\}\cdot\left\langle\Theta_1\right\rangle\cdot d\bar{y}_1-\int_{0}^{l_2}\kappa_1\cdot\left\{\Theta_2\right\}\cdot\left\langle\Theta_2\right\rangle\cdot d\bar{y}_2 \tag{70}$$

$$\left[K_{62}^{A}\right]=\int_{0}^{l_1}\left\{\Theta_1\right\}\cdot\left\langle\Theta_1\right\rangle\cdot d\bar{y}_1+\int_{0}^{l_2}\left\{\Theta_2\right\}\cdot\left\langle\Theta_2\right\rangle\cdot d\bar{y}_2 \tag{71}$$

$$\left[K_{66}^{A}\right]=-\int_{0}^{l_1}\kappa_2\cdot\left\{\Theta_1\right\}\cdot\left\langle\Theta_1\right\rangle\cdot d\bar{y}_1-\int_{0}^{l_2}\kappa_2\cdot\left\{\Theta_2\right\}\cdot\left\langle\Theta_2\right\rangle\cdot d\bar{y}_2 \tag{72}$$

$$\left[P_{11}^{A}\right]=\left\{\begin{array}{l}\int_{0}^{l_1} 2\cdot\pi\cdot\rho_{\infty}\cdot U_{\infty}\cdot\sin\left(\theta-\Lambda_1\right)\cdot\dot{\psi}\left(t\right)\cdot\bar{b}_1\cdot\left\{\Psi_1\right\}\cdot\left\langle\Psi_1\right\rangle\cdot d\bar{y}_1 \\ +\int_{0}^{l_2} 2\cdot\pi\cdot\rho_{\infty}\cdot U_{\infty}\cdot\sin\left(\theta-\Lambda_2\right)\cdot\dot{\psi}\left(t\right)\cdot\bar{b}_2\cdot\left\{\Psi_2\right\}\cdot\left\langle\Psi_2\right\rangle\cdot d\bar{y}_2\end{array}\right\} \tag{73}$$

$$\left[P_{12}^{A}\right]=\left\{\begin{array}{l}-\int_{0}^{l_1} 2\cdot\pi\cdot\rho_{\infty}\cdot U_{\infty}\cdot\sin\left(\theta-\Lambda_1\right)\cdot\dot{\psi}\left(t\right)\cdot\bar{b}_1^{2}\cdot\left(\frac{1}{2}-\bar{a}_1\right)\cdot\left\{\Psi_1\right\}\cdot\left\langle\Theta_1\right\rangle\cdot d\bar{y}_1 \\ -\int_{0}^{l_2} 2\cdot\pi\cdot\rho_{\infty}\cdot U_{\infty}\cdot\sin\left(\theta-\Lambda_2\right)\cdot\dot{\psi}\left(t\right)\cdot\bar{b}_2^{2}\cdot\left(\frac{1}{2}-\bar{a}_2\right)\cdot\left\{\Psi_2\right\}\cdot\left\langle\Theta_2\right\rangle\cdot d\bar{y}_2\end{array}\right\} \tag{74}$$

$$\left[P_{21}^{A}\right]=\left\{\begin{array}{l}\int_{0}^{l_1} 2\cdot\pi\cdot\rho_{\infty}\cdot U_{\infty}\cdot\sin\left(\theta-\Lambda_1\right)\cdot\dot{\psi}\left(t\right)\cdot\bar{b}_1\cdot\bar{e}_1\cdot\left\{\Theta_1\right\}\cdot\left\langle\Psi_1\right\rangle\cdot d\bar{y}_1 \\ +\int_{0}^{l_2} 2\cdot\pi\cdot\rho_{\infty}\cdot U_{\infty}\cdot\sin\left(\theta-\Lambda_2\right)\cdot\dot{\psi}\left(t\right)\cdot\bar{b}_2\cdot\bar{e}_2\cdot\left\{\Theta_2\right\}\cdot\left\langle\Psi_2\right\rangle\cdot d\bar{y}_2\end{array}\right\} \tag{75}$$

$$\left[P_{22}^{A}\right]=\left\{\begin{array}{l}-\int_{0}^{l_1} 2\cdot\pi\cdot\rho_{\infty}\cdot U_{\infty}\cdot\sin\left(\theta-\Lambda_1\right)\cdot\dot{\psi}\left(t\right)\cdot\bar{b}_1^{2}\cdot\bar{e}_1\cdot\left(\frac{1}{2}-\bar{a}_1\right)\cdot\left\{\Theta_1\right\}\cdot\left\langle\Theta_1\right\rangle\cdot d\bar{y}_1 \\ -\int_{0}^{l_2} 2\cdot\pi\cdot\rho_{\infty}\cdot U_{\infty}\cdot\sin\left(\theta-\Lambda_2\right)\cdot\dot{\psi}\left(t\right)\cdot\bar{b}_2^{2}\cdot\bar{e}_2\cdot\left(\frac{1}{2}-\bar{a}_2\right)\cdot\left\{\Theta_2\right\}\cdot\left\langle\Theta_2\right\rangle\cdot d\bar{y}_2\end{array}\right\} \tag{76}$$

As the structure's equation of motion is temporally dependent, the p-method is employed to derive the flutter speed. By accounting for the variable change of $\{\dot{q}\}=\{Y_1\}$, the equation of motion is reduced by one order, yielding the following expression.

$$\begin{array}{l}\{\dot{q}\}=\{Y_1\} \\ [M]\cdot\{\dot{Y}_1\}+[C]\cdot\{Y_1\}+[K]\cdot\{q\}=\{0\}\end{array} \tag{77}$$

And

$$\begin{bmatrix}[0] & [I] \\ [M] & [0]\end{bmatrix}\cdot\begin{Bmatrix}\{\dot{Y}_1\} \\ \{\dot{q}\}\end{Bmatrix}+\begin{bmatrix}-[I] & [0] \\ [C] & [K]\end{bmatrix}\cdot\begin{Bmatrix}\{Y_1\} \\ \{q\}\end{Bmatrix}=\{0\} \tag{78}$$

$$\left[M^{*}\right]\cdot\left\{\dot{q}^{*}\right\}+\left[K^{*}\right]\cdot\left\{q^{*}\right\}=\{0\}$$

Where

$$\left[M^{*}\right]=\begin{bmatrix}[0] & [I] \\ [M] & [0]\end{bmatrix},\qquad \left[K^{*}\right]=\begin{bmatrix}-[I] & [0] \\ [C] & [K]\end{bmatrix} \tag{79}$$

$$\left\{q^{*}\right\}=\begin{Bmatrix}\{Y_1\} \\ \{q\}\end{Bmatrix}$$

The generalized coordinates of p can be written as size and phase as follows.

$$\{q^*\} = \{\bar{q}\} \cdot e^{p \cdot t} \tag{80}$$

As a result, it can be written:

$$\begin{aligned} &\left(p \cdot \left[M^*\right] + \left[K^*\right]\right) \cdot \{\bar{q}\} \cdot e^{p \cdot t} = \{0\} \quad \Rightarrow \\ &\left(p \cdot \left[M^*\right] + \left[K^*\right]\right) \cdot \{\bar{q}\} = \{0\} \ \Rightarrow \\ &p \cdot \left[M^*\right] \cdot \{\bar{q}\} = -\left[K^*\right] \cdot \{\bar{q}\} \end{aligned} \tag{81}$$

Finally, for the eigenvalue p:

$$p \cdot \left[M^*\right] \cdot \{\bar{q}\} = -\left[K^*\right] \cdot \{\bar{q}\} \tag{82}$$

The eigenvalues of the matrix $\left[M^*\right]$ and $-\left[K^*\right]$, which are the values of p, have a real part and an imaginary part $p = \sigma + i \cdot \omega$. The imaginary part ω represents the frequency of the airflow. The flutter phenomenon occurs when the frequency of the airflow becomes equal to the structure and the real part σ becomes zero. In other words, the value of σ changes sign at the flutter speed.

5- Results and discussion

This section addresses determining the flutter speed of the double-sweep folding wing operating within a subsonic flow regime at sea level. The wing configuration comprises two distinct segments, as delineated in Figure 3: the first segment affixes to the body, and the second positions away from the body. The first segment exhibits a taper ratio, resulting in the linear variation of all mechanical and geometric properties across the airfoil cross-section. Conversely, the second segment lacks a taper ratio, maintaining consistent mechanical and geometric properties. The wing is fabricated of aluminum alloy, and Table 1 details its mechanical and geometric attributes. The plots illustrating the real and imaginary parts of the eigenvalues, derived from the Wagner and Kussner functions, are depicted in Fig. 4 to Fig. 7, respectively, facilitating the determination of flutter speed and frequency.

Table 1. The mechanical and geometric properties of the double-sweep folding wing.

Parameters	First segment	Parameters	Second segment
ρ_∞	1.225 kg/m^3	ρ_∞	1.225 kg/m^3
ρ_{Al}	2700 kg/m^3	ρ_{Al}	2700 kg/m^3
Λ_1	35°	Λ_2	40°
l_1	1 m	l_2	1 m
$\bar{b}_1(\bar{y})$	$0.19-0.069\cdot\bar{y}$	$\bar{b}_2$	0.5 m
$\bar{m}_1$	0.75 kg/m	$\bar{m}_2$	0.75 kg/m
$\bar{e}_1(\bar{y})$	$0.081-0.035\cdot\bar{y}$	$\bar{e}_2$	0.04
$\bar{a}_1(\bar{y})$	$\frac{e_1(\bar{y})}{b_1(\bar{y})}-\frac{1}{2}$	$\bar{a}_2$	0
$\bar{x}_{\alpha_1}$	$\frac{0.01}{b_1(\bar{y})}$	$\bar{x}_{\alpha_2}$	0.29
$\bar{I}_{\alpha_1}$	$0.203-0.168\cdot\bar{y}$ kg·m	$\bar{I}_{\alpha_2}$	0.1 kg.m
EI_1	$39535.238-28663.861\cdot\bar{y}$ N·m^2	EI_2	$2\times10^4\,N\cdot m^2$
GJ_1	$1950390.284-1612753.13\cdot\bar{y}$ N·m^2	GJ_2	$1\times10^4\,N\cdot m^2$

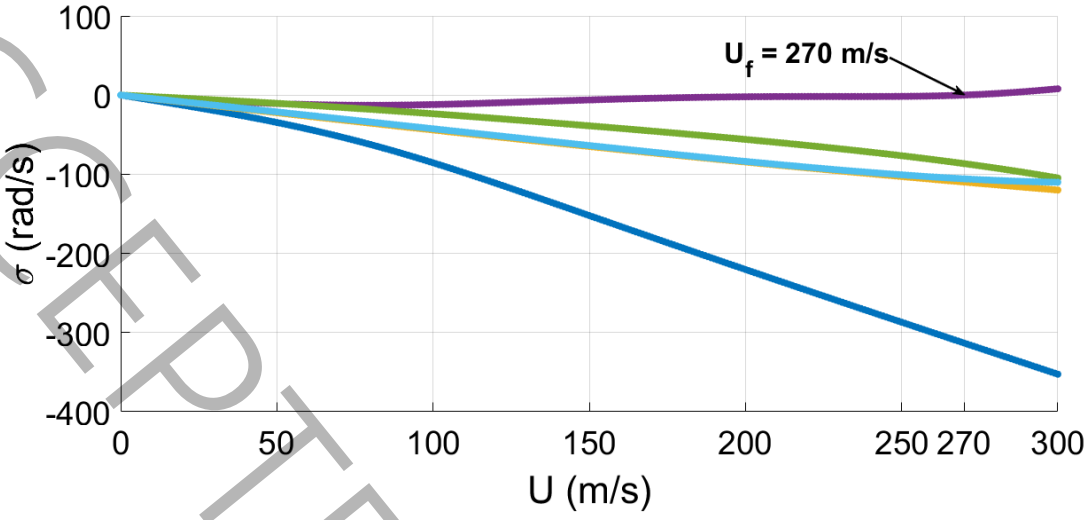

Fig. 4. The real part of the eigenvalues versus the airflow speed at the sea level based on Wagner's function

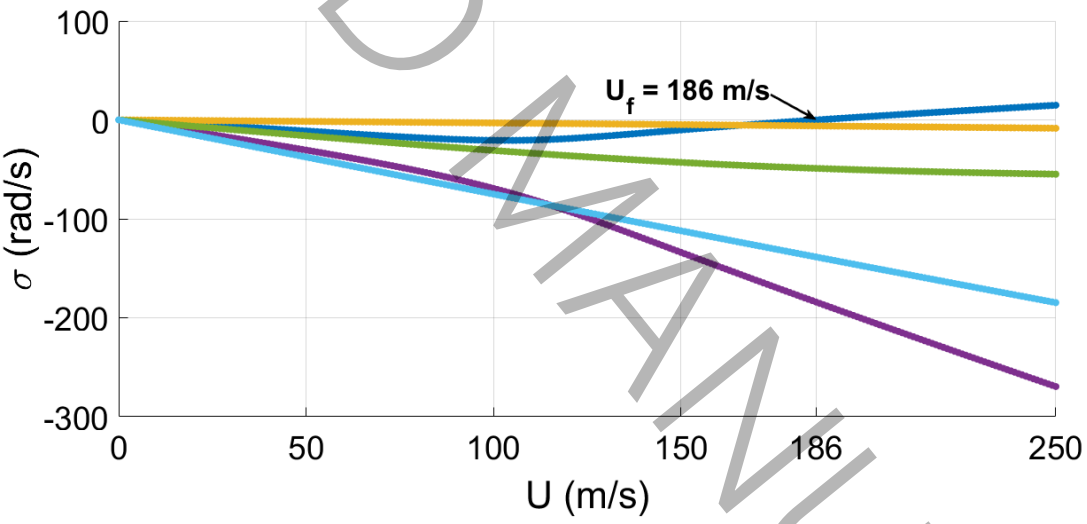

Fig. 5. The real part of the eigenvalues versus the airflow speed at the sea level based on Kussner's function

Each branch in Fig. 4 or Fig. 5 illustrates the variations in the real part of the eigenvalue to changes in airflow speed. The eigenvalue is derived from Eq. (82). Five branches are plotted for three mode shapes. The branch that starts from zero, initially moves towards negative values, and then shifts towards positive values is considered the branch that determines the flutter speed. The point where this branch changes sign from negative to positive is identified as the point where the flutter phenomenon occurs. The airflow speed at this intersection is equal to the flutter speed, where the

frequencies of the airflow and the structure are equal. According to Fig. 4 and Fig. 5, the flutter speeds obtained from the Wagner and the Kussner functions are 270 m/s and 186 m/s, respectively.

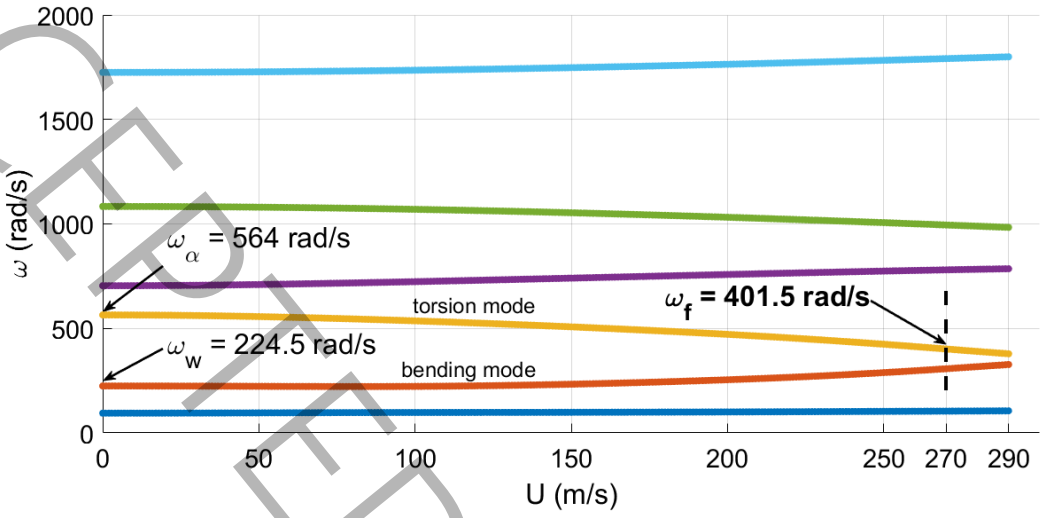

Fig. 6. The imaginary part of the eigenvalues versus the airflow speed at the sea level based on Wagner's function

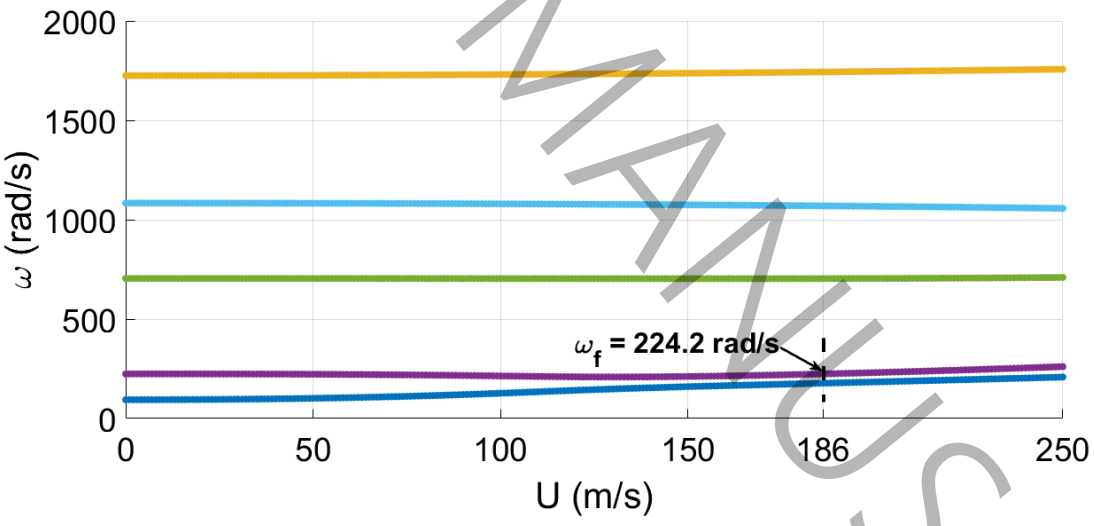

Fig. 7. The imaginary part of the eigenvalues versus the airflow speed at the sea level based on Kussner's function

Similar to the real part, each branch in Fig. 6 or Fig. 7 represents the changes in the imaginary part of the eigenvalue to variations in airflow speed. At the flutter speed, the two branches that are close to each other and continue in parallel determine the flutter frequency. The lower branch indicates the bending frequency, while the higher branch indicates the torsion frequency. At the flutter speed, the frequency corresponding to the torsion mode is equal to the flutter frequency. The flutter

frequency obtained from the Wagner function is 401.5 rad/s, and from the Kussner function, it is 224.2 rad/s. The Table 2 compares the flutter instability speed extracted from these two functions.

Table 2. Comparison of flutter speed and frequency for Wagner's and Kussner's function.

Conversion functions	$U_f\,(m/s)$	$\omega_f\,(rad/s)$
Wagner function	270	401.5
Kussner function	186	224.2
Difference percentage (%)	36.8	56.7

The data presented in the Table 2 indicate that Kussner's function demonstrates greater accuracy in achieving a precise answer compared to Wagner's function. It can be inferred that, in scenarios where airflow speed fluctuates, Kussner's function should be employed to determine the flutter speed. To investigate the effect of sweep angles on flutter speed and frequency, a design of experiment was carried out using the response surface method. The flutter speed and frequency results for each step are provided in Table 3.

Table 3. Input and response variables of the design of experiment.

Run	Λ_1 (deg)	Λ_2 (deg)	V_f (m/s)	ω_f (rad/s)
1	0	50	233	226.425
2	0	30	176.5	206.248
3	40	60	255	252.643
4	60	0	230	229.737
5	30	0	191	211.157
6	50	20	170.5	216.913
7	0	0	152	199.738
8	20	40	187	220.735
9	60	40	193.5	226.6
10	30	20	166	211.97
11	20	60	272	261.167

The correlation matrix between the input and response variables was calculated and is shown in Table 4. As can be seen, changes in sweep angles Λ_1 and Λ_2 have the least and most positive effects on flutter speed and frequency, respectively.

Table 4. Correlation matrix of sweep angles, flutter speed and frequency.

	Λ_1 (deg)	Λ_2 (deg)	V_f (m/s)	ω_f (rad/s)
Λ_1 (deg)	1			
Λ_2 (deg)	-0.1183	1		
V_f (m/s)	0.1438	0.6382	1	
ω_f (rad/s)	0.2913	0.7292	0.9324	1

The results of Table 4 indicate that sweep angle two has a greater impact on flutter speed and frequency comparing sweep angle one. Thus, it can be concluded that in double or multi-sweep wings, the farther the sweep angle is from the fuselage, the greater its influence on flutter speed and frequency.

6- The conclusion

In this paper, the speed flutter of a double-sweep folding wing was calculated based on Wagner's function and Kussner's function using the p-method. The results are as follows.

- The Kussner's function is commonly applied in cases of variable airflow. The airflow changes during the wing's deployment since the wing opens at high speed within a few seconds. In this context, Wagner's function is unsuitable for addressing the problem. Consequently, the speed and frequency of the flutter derived from using the Wagner function exhibit significant differences compared to those obtained using the Kussner's function. None of the previous studies have employed the Kussner's function under these circumstances.
- A novel mathematical method has been employed to transform aerodynamic equations from the frequency to the time domain. This innovative approach has not been applied in any prior research and proves highly valuable in the field of aeroelasticity because it reduces the problem from a two-parameter state to a one-parameter state.
- Converting the frequency to the time field and reducing the problem to a single parameter will enhance the response speed.
- The impact of varying sweep angles on flutter speed was analyzed, providing valuable insights for designers to select appropriate sweep angles for UAVs, ultimately leading to an optimal design. Changes in sweep angles one and two have

the least (0.1438, 0.2913) and most (0.6382, 0.7292) positive effects on flutter speed and frequency, respectively.

- This paper examines the double-sweep wing configuration. The approach used is general, and the developed code is scalable, allowing for application to multi-sweep wing designs which improves designers' ability to design multi-sweep wings.

7- Nomenclature

$B_{\bar{\alpha}1}, B_{\bar{\alpha}2}$	The degrees of freedom of the mode space for the torsional mode
b	The half-chord of the double-sweep wing in the coordinate system (x,y,z)
$\bar{b}$	The half-chord of the double-sweep wing is perpendicular to the elastic axis of the wing
$\bar{b}\bar{a}$	The distance from the center of the elastic to the half-chord
$\bar{b}\bar{x}_{\alpha}$	The distance from the center of mass to the elastic center
C	Aeroelastic damping matrix
C^S	Structural damping matrix
C^A	Aerodynamic damping matrix
d, κ_1, κ_2	Kussner function parameters
$\overline{EI}$	Bending stiffness of the wing
$\bar{e}$	The distance from the elastic center of the double-sweep wing to the aerodynamic center
$\bar{I}_{\alpha}$	The mass moment of a double-sweep wing per unit length
$\overline{GJ}$	Torsional stiffness of the wing
K	Aeroelastic stiffness matrix
K^A	Aerodynamic stiffness matrix
K^S	Structural stiffness matrix
k_f	Dimensionless frequency flutter
M	Aeroelastic mass matrix
M^A	Aerodynamic mass matrix
$\bar{M}_{e.a}$	Aerodynamic moment around the elastic center

M_f	Flutter mach number
M^S	Structural mass matrix
$\bar{m}$	Wing mass of double-sweep per unit of wing length
P	Initial condition matrix
q	Total generalized coordinates
r_w	Generalized coordinates of bending degree of freedom
r_{w_1}, r_{w_2}	Generalized coordinates of bending mode space
$r_{\bar{\alpha}}$	Generalized coordinates of torsional degrees of freedom
$r_{\bar{\alpha}_1}, r_{\bar{\alpha}_2}$	Generalized coordinates of torsion mode space
T	Kinetic energy
t	time dimension
U	Strain energy
$\bar{U}$	Velocity of flow perpendicular to the leading edge of double-sweep wing
U_f	Flutter speed instability
U_∞	The speed of the free air flow in the direction of the bird's movement
W_{ext}	The work of aerodynamic forces
w	Bending degree of freedom
$w_{a^{3c}/_4}$	Downwash function
(x, y, z)	Cartesian coordinate system
$(\bar{x}, \bar{y}, z)$	Double-sweep wing coordinate system
$\bar{\alpha}$	Torsional degree of freedom
Θ	Torsion mode shape
Λ	sweep angle
ρ_∞	Free air density
τ	Dimensionless time

χ, β	Values of shape parameters of bending mode
Ψ	Bending mode shape
$\psi(t)$	Kussner function
ω_f	Flutter frequency

8- References

[1] D. Borglund, The mu-k method for robust flutter solutions, Journal of aircraft, 41 (2004) 1209-1216.
[2] N. Rajamurugu, M. Satyam, V. Manoj, V. Nagendra, S. Yaknesh, M. Sundararaj, Investigation of Static Aeroelastic Analysis and Flutter Characterization of a Slender Straight Wing, International Journal of Automotive and Mechanical Engineering, 21(2) (2024) 11203-11219.
[3] L. Zhang, Y. Zhao, Time-Varying Aeroelastic Modeling and Analysis of a Rapidly Morphing Wing, Aerospace, 10(2) (2023) 197.
[4] K. Dhital, A.T. Nguyen, J.-H. Han, Aeroelastic modeling and analysis of wings in proximity, Aerospace Science and Technology, 130 (2022) 107955.
[5] T. Farsadi, M. Rahmanian, A. Kayran, Reduced order nonlinear aeroelasticity of swept composite wings using compressible indicial unsteady aerodynamics, Journal of Fluids and Structures, 92 (2020) 102812.
[6] A. Mazidi, S. Fazelzadeh, Aeroelastic modeling and flutter prediction of swept wings carrying twin powered engines, Journal of Aerospace Engineering, 26(3) (2013) 586-593.
[7] S. Sina, T. Farsadi, H. Haddadpour, Aeroelastic stability and response of composite swept wings in subsonic flow using indicial aerodynamics, Journal of Vibration and Acoustics, 135(5) (2013) 14.
[8] S.A. Fazelzadeh, P. Marzocca, A. Mazidi, E. Rashidi, Divergence and flutter of shear deformable aircraft swept wings subjected to roll angular velocity, Acta mechanica, 212 (2010) 151-165.
[9] W.-w. Zhang, Z. Ye, Effects of leading-edge vortex on flutter characteristics of high sweep angle wing, Hangkong Xuebao/Acta Aeronautica et Astronautica Sinica, 30(12) (2009) 2263-2268.
[10] R.K. Kapania, J.C. Issac, Sensitivity analysis of aeroelastic response of a wing in transonic flow, AIAA journal, 32(2) (1994) 350-356.
[11] R.H. Ricketts, R.V. Doggett, Jr., Wind-tunnel Experiments on Divergence of Forward-swept Wings, NASA Technical Paper 1685 NASA Langley Research Center and National Technical Information Service, (1980) 46.
[12] J. Mahig, Effect of Sweep Angle and Drag on the Flutter Speed of Hydrofoils, Journal of Hydronautics, 7(3) (1973) 104-108.
[13] R.D. Firouz-Abadi, M.R. Borhan Panah, Development of an aeroelastic model based on system identification using boundary elements method, Aircraft Engineering and Aerospace Technology, 94(3) (2022) 360-371.
[14] N. Akshayraj, A. Sriram, Effect of Wing Geometric Parameters on Flutter Speed, International Journal of Vehicle Structures & Systems, 14(1) (2022) 121-127.
[15] J.R. Kwon, R. Vepa, Transonic small disturbance unsteady potential flow over very high aspect ratio wings, The Aeronautical Journal, 126(1305) (2022) 1834-1852.
[16] G.M. Polli, L. Librescu, F. Mastroddi, Aeroelastic response of composite aircraft swept wings impacted by a laser beam, AIAA journal, 44(2) (2006) 382-391.
[17] A. Ghasemikaram, A. Mazidi, S.A. Fazelzadeh, D. Scholz, Flutter Analysis of a 3D Box-Wing Aircraft Configuration, International Journal of Structural Stability and Dynamics, 22(02) (2021) 2250016.
[18] S.A. Fazelzadeh, M. Rezaei, A. Mazidi, Aeroelastic analysis of swept pre-twisted wings, Journal of Fluids and Structures, 95 (2020) 103001.
[19] A. Alizadeh, Z. Ebrahimi, A. Mazidi, S.A. Fazelzadeh, Experimental nonlinear flutter analysis of a cantilever wing/store, International Journal of Structural Stability and Dynamics, 20(07) (2020).

[20] Y. Xiao, X. Wang, B. Huang, Analysis of flutter characteristics of swept wing, in: Seventh International Conference on Electromechanical Control Technology and Transportation (ICECTT 2022), SPIE, 2022, pp. 32-37.
[21] M. Basiri, H. Farrokhfal, M. Mosayebi, R. Koohi, Rapid Subsonic Flutter Analysis for Low Aspect Ratio Composite Wings, Iranian Journal of Mechanical Engineering Transactions of the ISME, 23(1) (2022) 68-86.
[22] A. Arun Kumar, A.K. Onkar, Frequency Domain Based Robust Flutter Analysis of Swept Back Wing Using μ Method, in: Recent Advances in Computational Mechanics and Simulations: Volume-II: Nano to Macro, Springer, 2020, pp. 609-622.
[23] S. Kumar, A.K. Onkar, M. Manjuprasad, Stochastic modeling and reliability analysis of wing flutter, Journal of Aerospace Engineering, 33(5) (2020).
[24] J. Melvin, W. Zhao, A Jacobi-Ritz Approach for Flutter Analysis of Swept Distributed Propulsion Aircraft Wing, in: ASME Aerospace Structures, Structural Dynamics, and Materials Conference, American Society of Mechanical Engineers, 2023, pp. V001T002A002.
[25] S. Liska, E.H. Dowell, Continuum aeroelastic model for a folding-wing configuration, AIAA Journal, 47 (2009) 2350-2358.
[26] Y. Zhao, H. Hu, Parameterized aeroelastic modeling and flutter analysis for a folding wing, Journal of Sound and Vibration, 331 (2012) 308-324.
[27] S. Shams, M. Keshtgar, M. Mansouri, Aeroelastic Analysis of a Double-Sweep Wing with the Metal/Composite Sections, Modares Mechanical Engineering, 19 (2019) 927-935.
[28] K.-N. Koo, Aeroelastic characteristics of double-swept isotropic and composite wings, Journal of aircraft, 38 (2001) 343-348.
[29] P. Marzocca, L. Librescu, W.A. Silva, Aeroelastic response and flutter of swept aircraft wings, AIAA journal, 40 (2002) 801-812.
[30] A. Mazidi, S.A. Fazelzadeh, Flutter of a swept aircraft wing with a powered engine, Journal of Aerospace Engineering, 23 (2010) 243-250.
[31] R.D. Firouz-Abadi, A.R. Askarian, P. Zarifian, Effect of thrust on the aeroelastic instability of a composite swept wing with two engines in subsonic compressible flow, Journal of Fluids and Structures, 36 (2013) 18-31.
[32] S.A. Sina, T. Farsadi, H. Haddadpour, Aeroelastic Stability and Response of Composite Swept Wings in Subsonic Flow Using Indicial Aerodynamics, Journal of Vibration and Acoustics, 135(5) (2013).
[33] H.R. Ovesy, A. Nikou, H. Shahverdi, Flutter analysis of high-aspect-ratio wings based on a third-order nonlinear beam model, Proceedings of the Institution of Mechanical Engineers, Part G: Journal of Aerospace Engineering, 227(7) (2012) 1090-1100.
[34] K. Jacobson, B. Stanford, S. Wood, W.K. Anderson, Flutter Analysis with Stabilized Finite Elements based on the Linearized Frequency-domain Approach, in: AIAA SciTech 2020 Forum, 2020, pp. 403.
[35] J. Shi, D. Hitchings, Calculation of flutter derivatives and speed for 2-D incompressible flow by the finite-element method, Applied mathematical modelling, 18 (1994) 538-549.
[36] R.L. Bisplinghoff, H. Ashley, R.L. Halfman, Aeroelasticity, Second ed., Dover Publications, 2013.
[37] D.H. Hodges, G.A. Pierce, Introduction to Structural Dynamics and Aeroelasticity, Second ed., Cambridge University Press, 2012.
[38] H. Dowell, A Modern Course in Aeroelasticity, Springer International Publishing, 2021.
[39] P. Marzocca, L. Librescu, W.A. Silva, Unified Formulation of the Aeroelasticity of Swept Lifting Surfaces, Virginia Polytechnic Institute and State University and NASA Langley Research Center, (2001) 34.